To the Graduate Council:

I am submitting herewith a thesis written by David L. Conner entitled "The Design and Testing of a Cam Timing Delay Mechanism for High Performance Combustion Engines." I have examined the final copy of this thesis for form and content and recommend that it be accepted in partial fulfillment of the requirements for the degree of Master of Science, with a major in Mechanical Engineering.

Frank H. Speckhart
Major Professor

We have read this thesis and recommend its acceptance:

Accepted for the Council:

Vice Provost and
Dean of The Graduate School

STATEMENT OF PERMISSION TO USE

In presenting this thesis in partial fulfillment of the requirements for a Master of Science degree at The University of Tennessee, Knoxville, I agree that the Library shall make it available to borrowers under rules of the Library. Brief quotations from this thesis are allowable without special permission, provided that accurate acknowledgment of source is made.

Permission for extensive quotation from or reproduction of this thesis may be granted by my major professor, or in his absence, by the Head of Interlibrary Services when, in the opinion of either, the proposed use of the material is for scholarly purposes. Any copying or use of the material in this thesis for financial gain shall not be allowed without my written permission.

Signature David L. Conner

Date April 24, 1989

THE DESIGN AND TESTING OF A CAM TIMING DELAY MECHANISM FOR HIGH PERFORMANCE COMBUSTION ENGINES

A Thesis

Presented for the

Master of Science

Degree

The University of Tennessee, Knoxville

David L. Conner

May 1989

I wish to dedicate this work to

my father C. F. Conner

for his encouragement in my

pursuit of an advanced degree.

ACKNOWLEDGMENTS

The author would like to express appreciation to Dr. Frank H. Speckhart for his guidance and constructive criticism during the preparation of this report. Thanks are extended to Dr. J. W. Hodgson for his input and help with the project. Special thanks are offered to Chris Moscone and Tom Costner for the use of their engine and parts, respectively.

ABSTRACT

The performance of a high speed combustion engine can be improved by changing the cam shaft timing relative to the crank shaft timing as a function of the engine speed. In general, the camshaft should be retarded as the engine speed increases. The purpose of this investigation was to design and test a mechanical cam-retarding mechanism which would meet as many of the desired specifications as possible.

Utilizing the computer to solve the response for various geometries, a conceptual design was developed and analyzed. Several types of springs were analyzed to select the stiffest, effective spring within the working stress which the space underneath the timing cover could accomodate. Stiff springs were required to decrease the torque sensitivity of the device. Consequently, high spring stresses limited the life of the proposed design. After the best physical geometry to minimize the torque dependency of the mechanism and the most effective spring had been determined, individual parts were designed. The cam retarder prototype, built to operate at lower than design speeds because of limited test facilities, was tested by employing a dynamometer to drive the test engine.

The experimental results of cam speed versus relative cam rotation matched those of the analytical study once the cam torque had been determined. It was discovered that the cam torque decreased to approximately one-third of its static value as the engine speed increased. The possibility of fitting the cam retarding mechanism underneath the stock timing cover of a Chevrolet engine was found to be unrealistic.

TABLE OF CONTENTS

CHAPTER		PAGE
1.	INTRODUCTION	1
	A. Background	1
	B. Problem Statement	3
	C. Objectives of the Study	4
2.	DESIGN APPROACH	7
	A. Survey of Previous Designs	7
	B. Selection of Design Concept	13
	C. Theoretical Analysis	14
	D. Optimum Geometry	16
	E. Spring Considerations and Analysis	20
3.	COMPONENT DESIGN	37
	A. Gear Preparation	37
	B. Arm Design	39
	C. Spacer and Drive Plate Design	43
	D. Fasteners	46
	E. Bearing Selection	46
	F. Spring Specifications	49
	G. Assembly	50
4.	PROTOTYPE DESIGN	54
5.	PROTOTYPE TESTING	63
	A. Experimental Set-up	63
	B. Testing Procedure	65
	C. Experimental Results and Comparison	65
	D. Sources of Error	70
6.	FAILURE ANALYSIS	74
	A. Analysis of Load Bearing Parts	74
	B. Consequences of Failure	74
7.	COST ANALYSIS	77

CHAPTER	PAGE
8. SUMMARY	80
A. Conclusions	80
B. Recommendations	81
LIST OF REFERENCES	82
APPENDIXES	84
A. Beam Stress Calculations	85
B. Theoretical Analysis	89
C. Part Failure Analysis	102
D. Computer Programs	105
VITA	115

LIST OF TABLES

TABLE		PAGE
1.	Parts List	51
2.	Spring Parameters	55
3.	Spring Test Data	55
4.	Experimental Data and Program Output	73
5.	Labor and Machining Cost	78
6.	Material Cost	78
7.	Prefabricated Part Cost	79
8.	Total Cost	79

LIST OF FIGURES

FIGURE		PAGE
1.	Cam timing lagging the crank shaft timing by a given phase angle	2
2.	Assembly view of the final cam retarder design	6
3.	Assembled cam retarder designed by Richard Moisan	8
4.	Torque sensitivity curves	9
5.	Conceptual design of a cam retarding mechanism by Dr. F.H. Speckhart	11
6.	Illustration of slot rotation	12
7.	Conceptual design of the cam retarding mechanism	15
8.	Illustration of the pivoting arm's geometrical variables	17
9.	Theoretical cam speed vs. cam rotation curves for zero friction in the mechanism	21
10.	Theoretical cam speed vs. cam rotation curves for varying amounts of friction	22
11.	Theoretical cam speed vs. cam rotation curves for varying cam torque with constant friction in the mechanism	23
12.	Free body diagram of the pivoting arm	24
13.	Inside gear dimensions	25
14.	Cantilever beam analytical model	26
15.	Configuration utilizing a cantilever beam .	26
16.	Configuration utilizing a straight beam ...	27
17.	Configuration utilizing a curved beam	28

FIGURE		PAGE
18.	Helical spring formed from round wire	30
19.	Possible compression spring applications ..	31
20.	Drawbar spring	32
21.	Conventional extension spring end loop	34
22.	Reduced diameter end turns to decrease end loop stress	34
23.	Estimated stress-life curve for round steel spring wire	36
24.	Basic dimensions of a stock timing gear for a 350 cu.in Chevrolet engine	38
25.	Cam timing gear detail drawing	40
26.	Pivot arm detail drawing	41
27.	Centroid location calculation	42
28.	Spacer orientation within the mechanism ...	44
29.	Graphical determination of the cam rotation for a given slot angle	45
30.	Drive plate detail drawing	47
31.	Spacer detail drawing	48
32.	Pivot pin and bearing shaft detail drawings	48
33.	Assembly view of the final cam retarder design	52
34.	Experimental spring rate curves	56
35.	Complete parts display of prototype mechanism	58
36.	Stock timing gear before and after machining	58

FIGURE		PAGE
37.	Gear and mounting plate assembly	59
38.	Spacer back side and front view	60
39.	Drive plate	61
40.	Pivot arm with and without bearing attached	61
41.	Assembled cam retarder timing configuration and standard timing gear	62
42.	Fabricated plexiglass timing cover mounted on the test engine	64
43.	Test set-up	66
44.	Rotation measurement increments	67
45.	Illustration of the moment created by the torque reaction force for a large slot angle	67
46.	Experimental and theoretical curves for the motion utilizing the 6 lb/in springs on the mechanism	71
47.	Experimental and theoretical curves for the motion utilizing the 9 lb/in springs on the mechanism	72
A-1.	Beam cross-section	86
A-2.	Free-body diagram	87
A-3.	Curved beam configuration	88
B-1.	Vectors defining the location of the center of mass	90
B-2.	Vectors defining minimum and maximum arm angle	91
B-3.	Spring deflection	93
B-4.	Vectors defining pin position	95

FIGURE		PAGE
B-5.	Vectors defining friction force and torque reaction force direction	96
B-6.	Vectors defining spring force direction ...	98
B-7.	Arm free body diagram	100
C-1.	Bearing shaft loading	103
C-2.	Pivot pin loading	104
C-3.	Cam shaft bolt pattern and spacing	104

LIST OF SYMBOLS AND ABBREVIATIONS

SYMBOL	DESCRIPTION	UNITS
β	Cam rotation angle	radians
$\vec{M}$	General moment vector	inch-pounds
$\vec{r}$	General position vector	inches
$\vec{F}$	General force vector	pounds
θ	Absolute arm angle	radians
Δ	Delta, change in variable	-----
K	Spring rate	pounds per inch
fo	Spring preload	pounds
R1	Distance from cam center to arm pivot point	inches
Lp	Distance from pivot point to pin	inches
Lcm	Distance from pivot point to center of mass	inches
LT	Distance from pivot point to spring connection	inches
μ	Coefficient of friction	-----
ω	Angular velocity	radians per second
f	Friction force	pounds
Ft	Torque reaction force	pounds
Fc	Centrifugal force	pounds
Fsp	Spring force	pounds

Ry	Reaction force on arm in Y-direction	pounds
Rx	Reaction force on arm in X-direction	pounds
P	Applied load	pounds
c	Spring index	-----
Ks	Shear stress factor	-----
τ	Shear stress	pounds per square inch
G	Shear modulus of elasticity	pounds per square inch
N	Number of active spring coils	-----
Nt	Total number of spring coils	-----
Ls	Solid height of spring	inches
Lf	Free length of spring	inches
y	Spring deflection	inches
d	Wire diameter	inches
D	Nominal spring diameter	inches
S(ult)	Ultimate stength	pounds per square inch
$\bar{x},\bar{y}$	Centroid location	inches
$	Dollars	-----
I	Area moment of inertia	inches^4
E	Modulus of elasticity	pounds per square inch
b	Beam width	inches
h	Beam thickness	inches
L	Beam length	inches
σ_b	Normal bending stress	pounds per square inch
T	Torque	inch-pounds
w	Distributed load	pounds per inch

ABBREVIATIONS

ID = Inside Diameter

OD = Outside Diameter

DIA = Diameter

FT = Feet

RPM = Revolutions Per Minute

DEG = Degrees

FBD = Free Body Diagram

PSI = Pounds Per Square Inch

LB = Pounds

IN = Inches

MAX = Maximum

MIN = Minimum

CU. IN. = Cubic Inches

TPI = Threads Per Inch

F.S. = Factor of Safety

CHAPTER 1

INTRODUCTION

A. Background

For many years engineers have worked to improve the performance of the internal combustion engine. Consequently, better materials, new engine configurations, and ingenious devices have been developed to enhance its overall performance. Before any of these innovations could evolve, extensive testing had to be done to define which engine characteristics would yield higher output. Through years of this research, it was discovered and proven that retarding the cam timing as the engine speed increased would increase power. This task can be accomplished by rotating the cam shaft a few degrees relative to the crank shaft. The delayed cam would then open and close the valves later.

The combustion efficiency is less than maximum at high speeds because a pressure drop develops across the valves. This pressure difference results in air being pulled into the cylinder with a large velocity. The intake valve usually closes while a column of air is still being drawn into the cylinder. Ideally, the valve would remain open until the air just begins to change direction and move up the

cylinder. The cam phasing technique, illustrated in Figure 1, proves advantageous by increasing the amount of air allowed into the cylinder at high speeds.

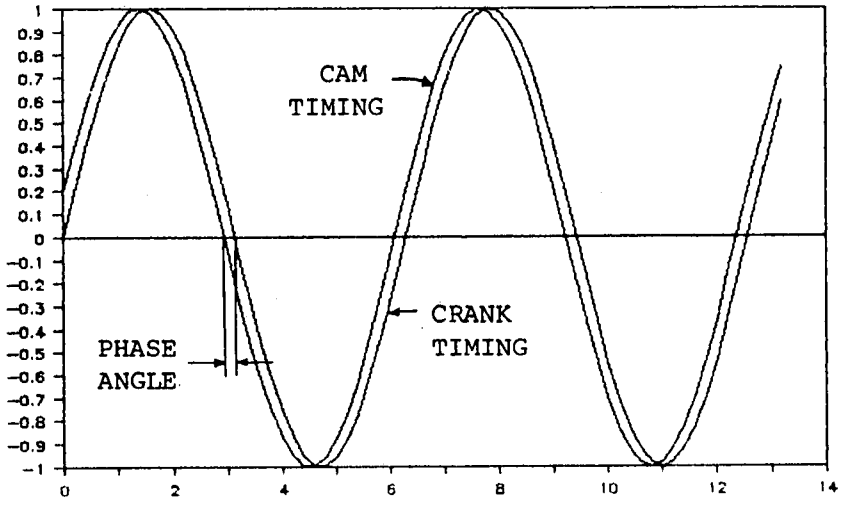


Figure 1. Cam timing lagging the crank shaft timing by a given phase angle.

Consequently, interest has been shown in the design of an engine with variable cam timing capabilities. Several attempts have been made at designing a retarding cam system to perform with accuracy and remain within the limits of economic feasibility. Two such mechanisms were designed at the University of Tennessee; one by mechanical engineering professor Frank Speckhart and one by ME student Richard Moisan. Both of these designs were powered and controlled by mechanical means only. Other systems could also be utilized in a design. For example, a British company has

developed a variable cam timing device making use of hydraulic power from the engine and electronic controls (see Reference 1).

B. Problem Statement

The problem undertaken in this thesis was to design and test a cam retarding device which would operate predictably and have an acceptable factor of safety. As in most engineering problems, there were requirements and specifications which had to be considered.

1. The mechanism was to be implemented on a standard Chevrolet V-8 engine. Because of this specification, space was the most constraining factor in the design. The lack of space under the standard timing cover limited the design to the interior and close proximity of the timing gear. This also confined the design to be a self-contained mechanism. Therefore, no hydraulic or electronic systems could be used.

2. It was desired to minimize the effect of the cam driving torque, caused by resistance of the valve springs, on the performance of the mechanism.

3. Specification for the relative rotation angle was 2°. The phase lag of the cam was to be a minimum of 2° behind the crank timing.

4. Specification for working speeds was 7100 to 7800 rpm crank shaft speed. It was also desired to develop a design where the working speeds could be varied by some means.

5. The last requirement was that the rotation be continuous between the starting and final working speeds given above. That is, the rotation would gradually increase with speed and the mechanism would not step or move suddenly from position to position.

C. Objectives of the Study

The effort to design a cam retarding device, which would conform to the above specifications and limitations, was organized to cover three main objectives:

1. To develop the force/dynamic analysis of all working parts to predict the behavior of the mechanism as a function of engine speed. Included in this study were hysteresis effects due to friction. Computer programs were developed in an attempt to optimize the geometry of the design.

2. To design and develop the completed mechanism. The design of parts, stress analysis, and bearing selection were some parts of this section. Several spring types were considered and analyzed in an effort to attain the lowest

stress situation. An assembly view of completed mechanism is shown in Figure 2.

3. To test and evaluate the prototype cam retarder. Testing of the device would be limited to electric motor driven engine conditions, since testing on an operating automobile engine was beyond the scope of the project. The prototype would to be designed to work at speeds much less than the design speeds due to equipment limitations and safety precautions. Comparison of the analytical and experimental results showed the accuracy of the analysis. Several sources of error in both calculation and testing could explain any discrepancies.

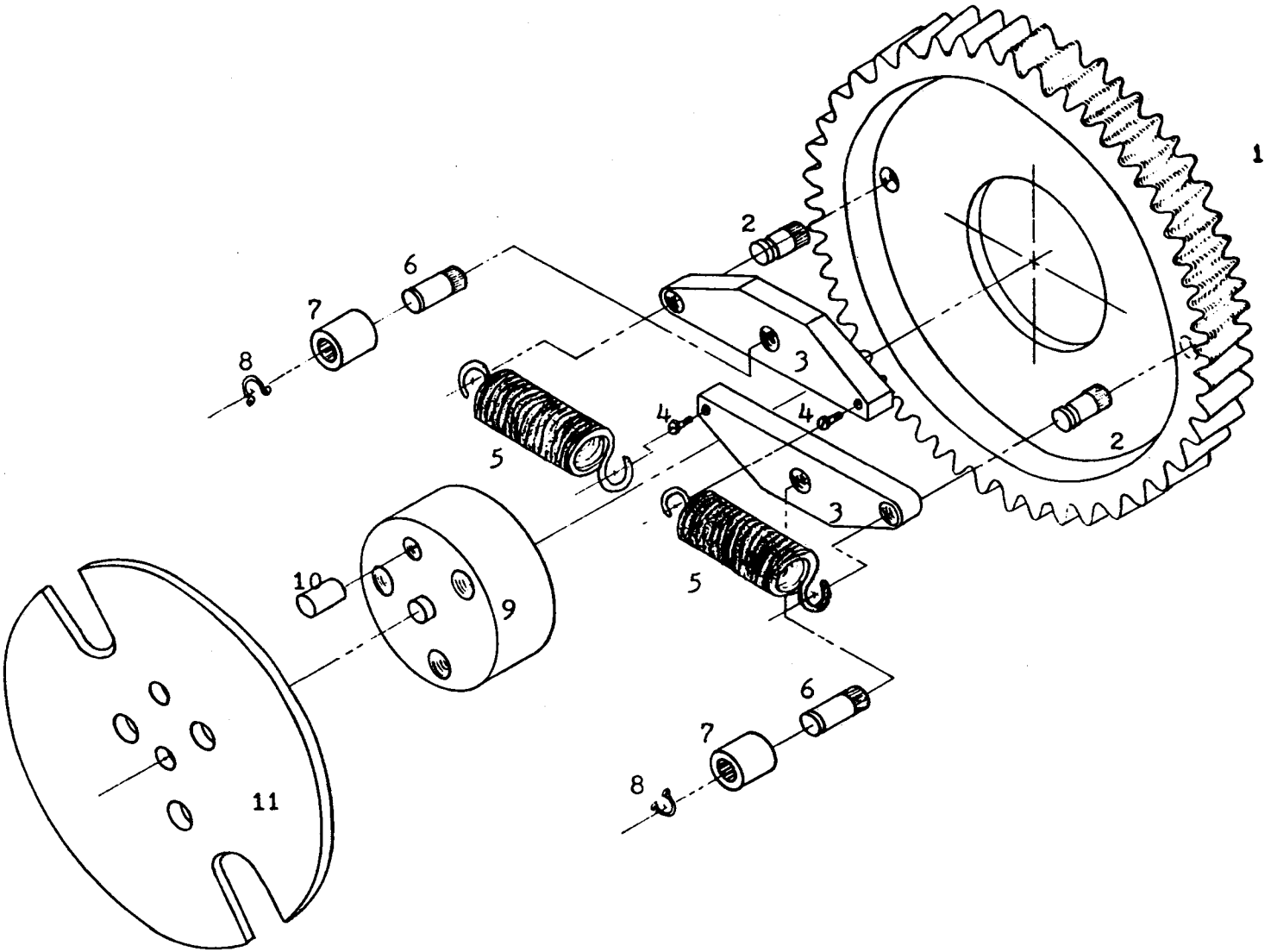


Figure 2. Assembly view of the final cam retarder design.

CHAPTER 2

DESIGN APPROACH

A. Survey of Previous Designs

In beginning a new design, the most obvious starting point is the study of previous similar design efforts. Studying previous designs allows the engineer to identify the varied methods that have been used to accomplish the specific task of the machine. The engineer can benefit by learning the advantages and disadvantages of each method. In this case, a literature search revealed some information on variable cam timing but no information on a totally mechanical cam retarding device. The two cam retarder designs mentioned previously were the only reference cases.

The first design considered was the work of an engineering student Richard Moisan. This cam delay mechanism, shown in Figure 3, is a spring loaded linkage system utilizing centrifugal force to move the preloaded link outward and rotate the cam relative to the crank shaft. The effect of pin joint friction on the mechanism's performance was unknown. Also, the torque dependency of the device was relatively large as seen in Figure 4. One can see that a 5 ft-lb. increase in cam torque at constant speed would change

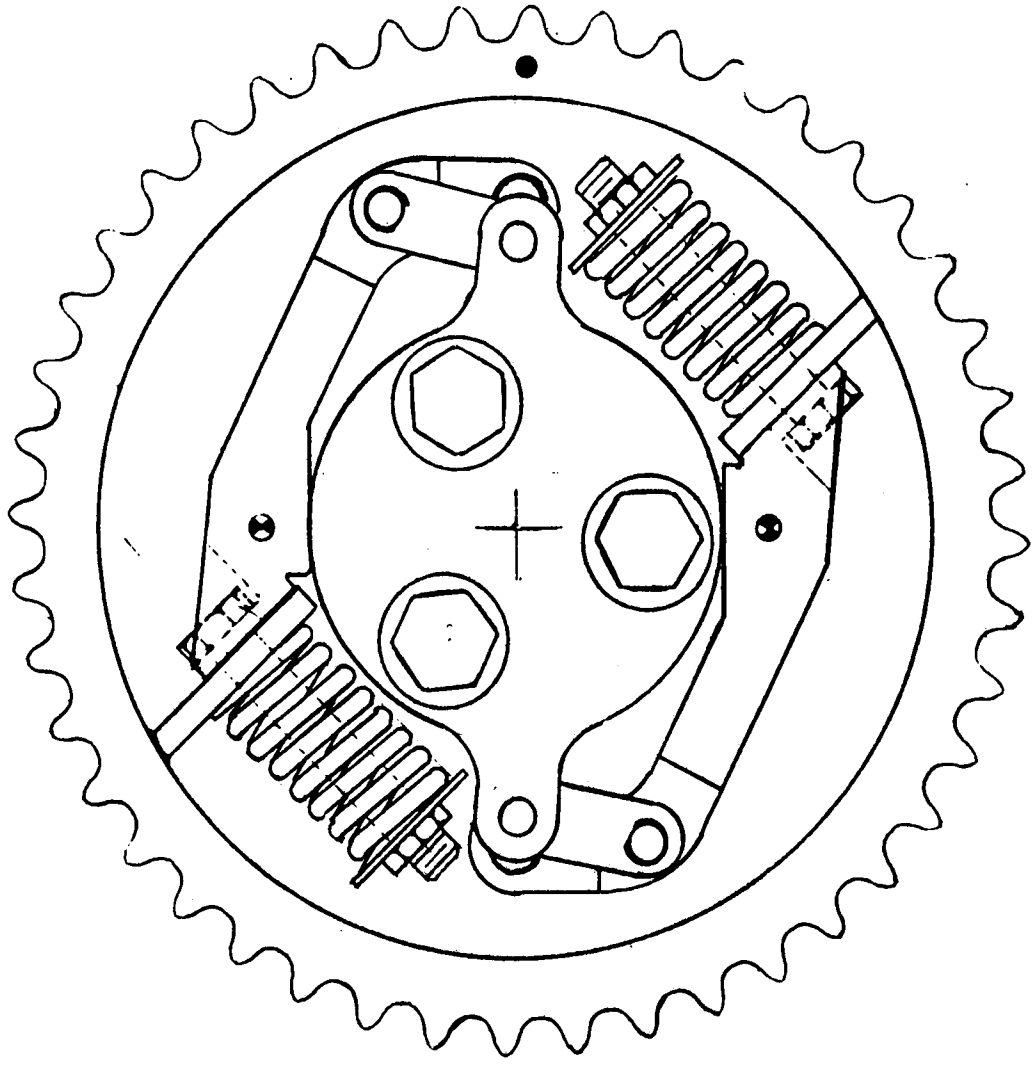


Figure 3. Assembled cam retarder designed by Richard Moisan.
Source: Richard Moisan, "Design of a Camshaft Gear for Variable Valve Timing in a 350 Cubic Inch Displacement Chevrolet High Performance Engine" (unpublished design project, The University of Tennessee, Knoxville, 1987), p. 17.

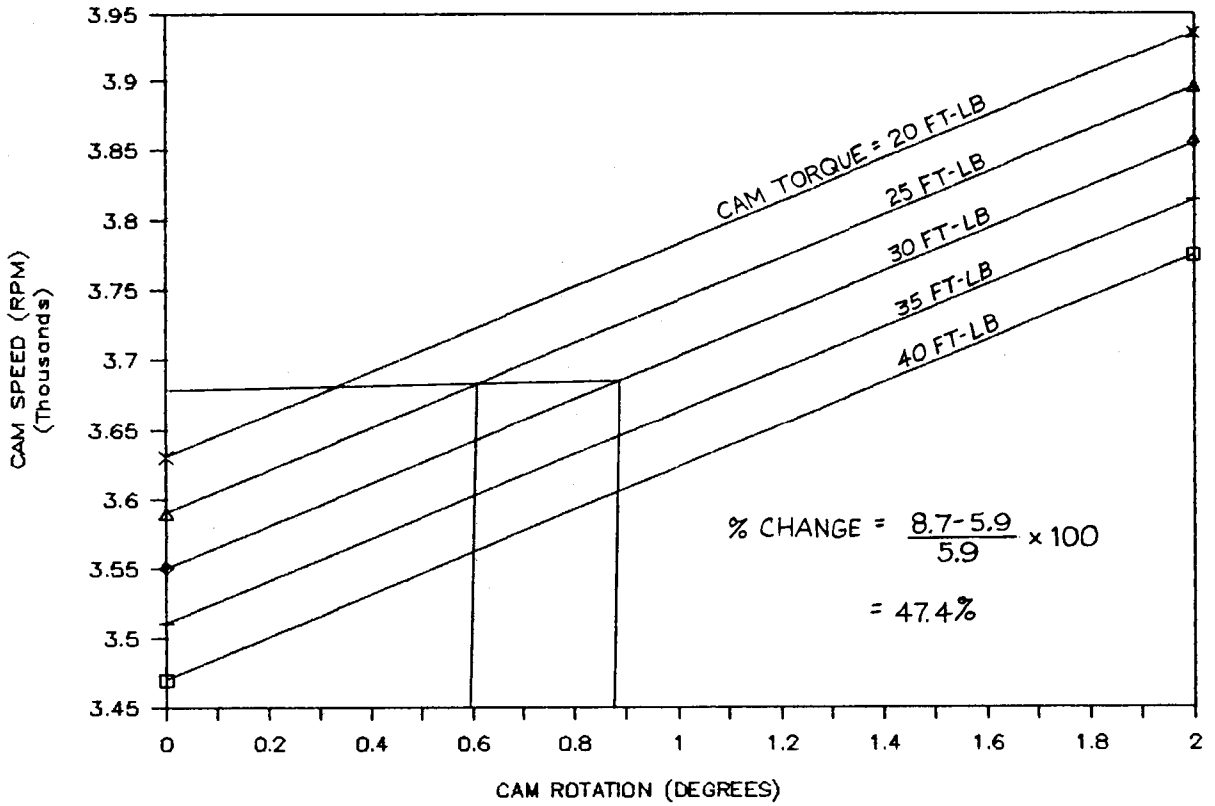


Figure 4. Torque Sensitivity Curves.
Source: Richard Moisan, "Design of a Camshaft Gear for Variable Valve Timing in a 350 Cubic Inch Displacement Chevrolet High Performance Engine" (unpublished design project, The University of Tennessee, Knoxville, 1987), p. 8.

the rotation 47.4%. No other problem with this design could be predicted from the given information.

Next, Dr. Speckhart's design was considered. A schematic provided in Figure 5 shows the pin and slot type design. The pins, connected to centrifugal weights turn with the crank shaft and move up the slots as speed increases. The slots, which are in a plate connected to the cam shaft, are angled relative to the movement of the pins. Therefore, the cam is rotated relative to the crank (see Figure 6). Although Dr. Speckhart has had some success with this design, some problems do exist. One is hysteresis due to friction between the pin and slot. The spring and centrifugal forces would have to be very large relative to the friction forces to reduce the hysteresis effect. This design would also have some torque dependency, although the exact amount was unknown.

After considering both of these designs, it became evident that the two major problems with any device of this type would be torque dependency and hysteresis. Later, it was discovered that springs would also be difficult to design because of high stresses.

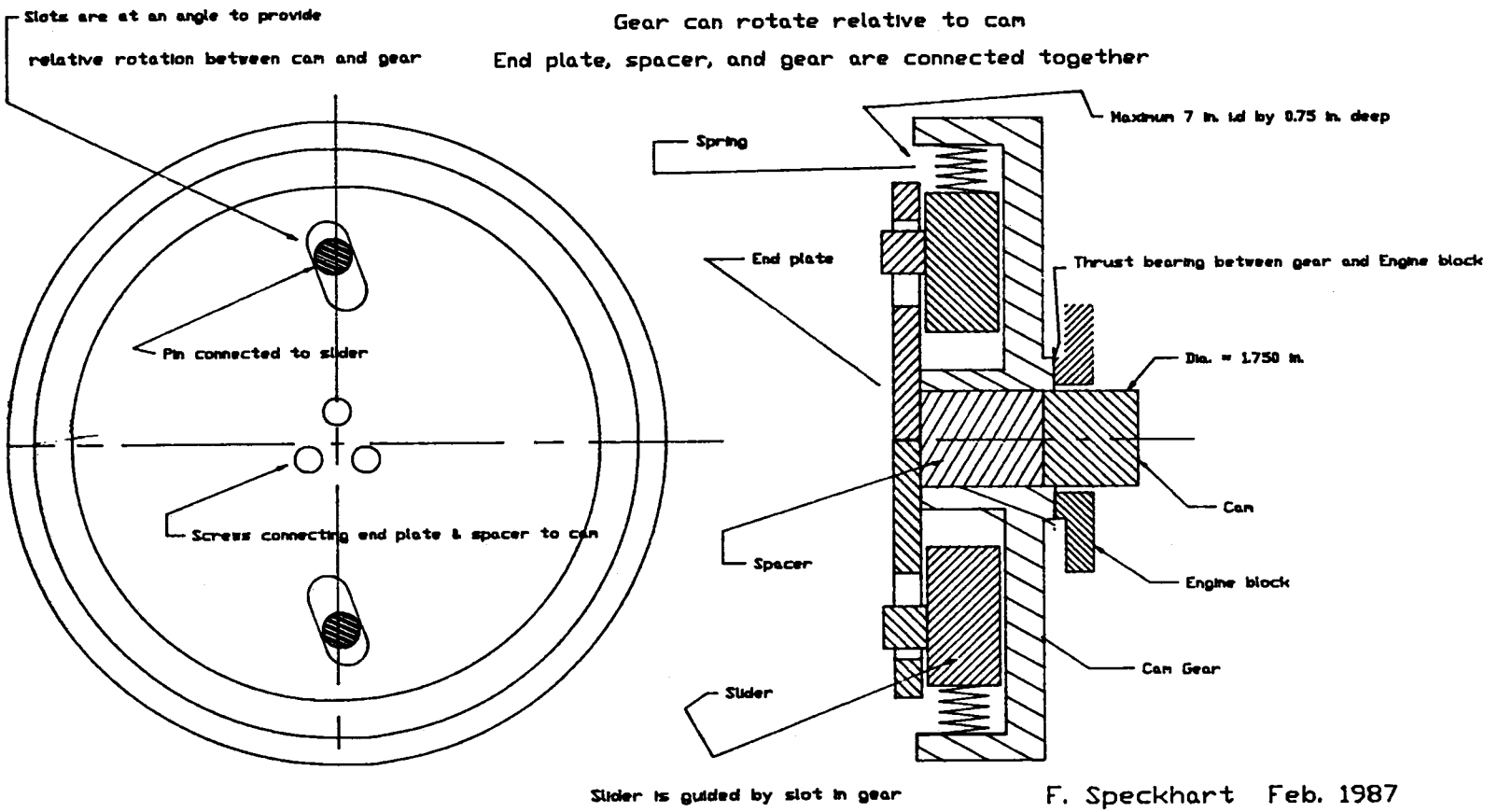


Figure 5. Conceptual design of a cam retarding mechanism by Dr. F.H. Speckhart. Source: Dr. F.H. Speckhart (unpublished design assignment, The University of Tennessee, 1987).

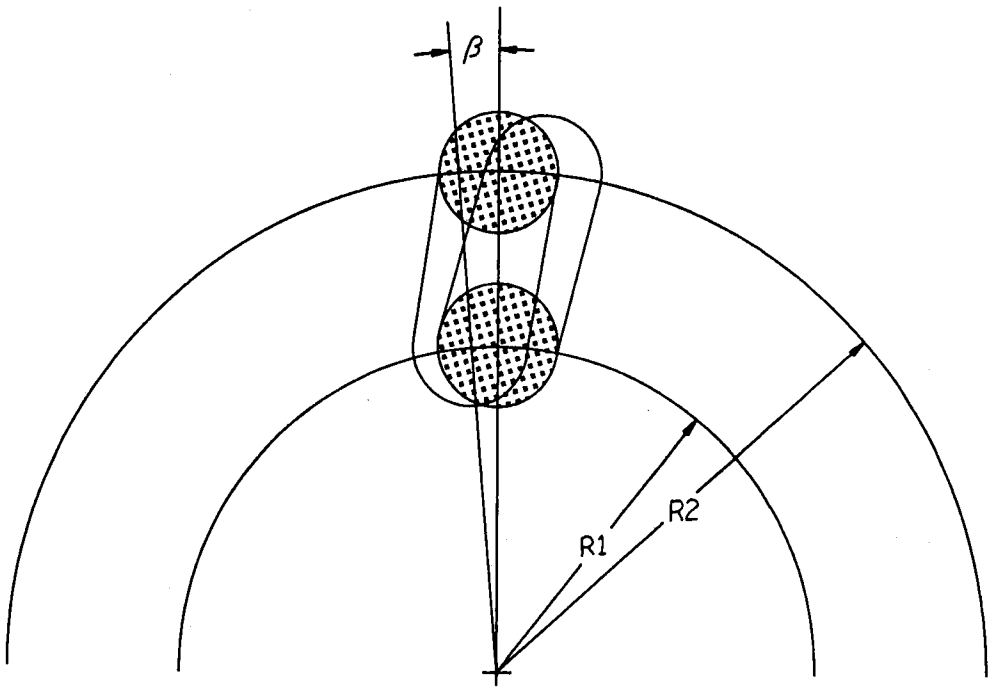


Figure 6. Illustration of slot rotation. The pin is confined to move from R1 to R2 along a radial line forcing the plate to rotate.

B. Selection of Design Concept

After eliminating several original ideas from consideration, a decision was made to use the pin and slot concept as a basis for the design. Reasons for this decision included simplicity of design, fewer friction surfaces and the possibility of using several different types of springs. The advantage of a simple design is it can be analyzed and fabricated with minimal error. The one friction surface between the pin and slot could be eliminated using rolling bearings. Therefore, hysteresis effects would no longer be a problem. The freedom to use different types of springs allows the designer to find the least stressed spring after analyzing each possibility. It was also believed that the torque dependency could be minimized by finding the optimum geometry for the centrifugal weights, pins and slots. Since the motion of the weights must follow a defined path, it was decided to have the weights pivot about a fixed point. This method would only add a frictional moment to the dynamic analysis of the link. If deemed necessary, this moment could be eliminated using another rolling element at the pivot point. Other methods, such as having the weight slide in a groove, would add unavoidable sliding friction to the analysis and, thus, bring hysteresis back into the mechanism. The geometry of the device made the decision to use

two symmetric weights and slots an obvious one. Using more would decrease the amount of the cam torque transmitted by each, but the space limitation would not allow for more than two. After all of these considerations had been made, the conceptual design for the cam retarding mechanism, shown in Figure 7, had been developed.

C. Theoretical Analysis

The theoretical dynamic analysis of the pivoting centrifugal weights was performed using vector notation. The direction of each position and force vector was stated in two-dimensional Cartesian coordinates. It would be preferred to calculate the position of the link directly as a function of cam speed, but this is a more difficult task. Each position and force vector is a nonlinear function of the angular position of the link, while the cam speed only effects the magnitude of the centrifugal force. Therefore, it is much simpler to set the position angle to a constant and solve for the cam speed rather than solving the nonlinear equations simultaneously for the position angle. Each moment about the pivot point is calculated using:

$$\vec{M} = \vec{r} \times \vec{F} \qquad (1)$$

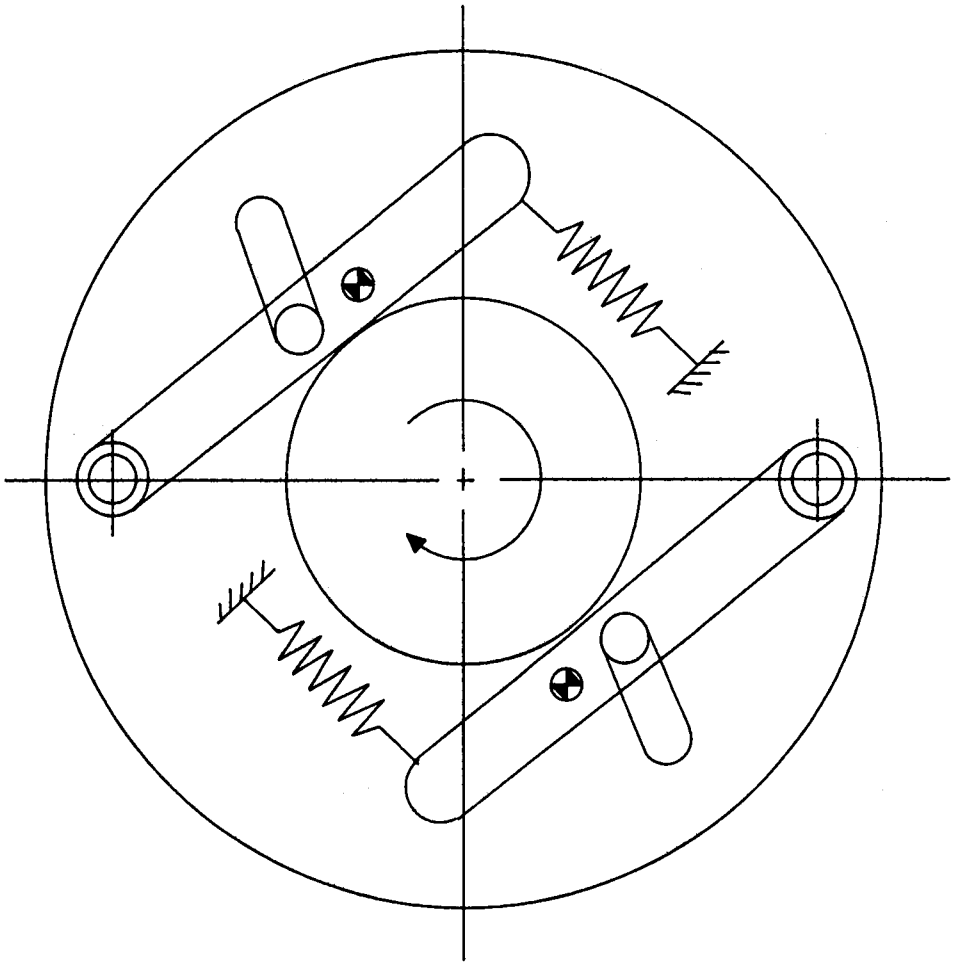


Figure 7. Conceptual design of the cam retarding mechanism.

where $\vec{r}$ = position vector relative to the pivot point

$\vec{F}$ = force vector

At this point in the analysis the link has no physical dimensions, only position vectors of specified points and a concentrated mass at the centroid. Each step of the analysis is given in Appendix B. Using this analysis, a logic flow chart and corresponding computer program, both found in Appendix D, were developed to perform the calculations.

D. Optimum Geometry

The goal of the analysis was to attain the geometry which would minimize the torque dependency and hysteresis of the motion. In an attempt to optimize the physical geometry of the device, five parameters were varied in the analysis program. The terms weight and arm are used interchangeably in the discussion.

1. The mass of the centrifugal weights was one variable. It was desired to use as large a weight as possible in order to make the centrifugal forces large compared to friction forces. Therefore, large weights would decrease hysteresis due to friction. The problem associated with using large weights was the required preload of the springs. The weight was limited by the largest usable spring which could produce the preload without being overstressed.

2. The distance from the center of the gear to the pivot point (R1) was another variable (refer to Figure 8 for illustration of variables). This distance was limited by the minimum and maximum radii of the working space. From studying the analytical output from the computer program, it was discovered that using the maximum radius from the center to the pivot would produce the smallest hysteresis.

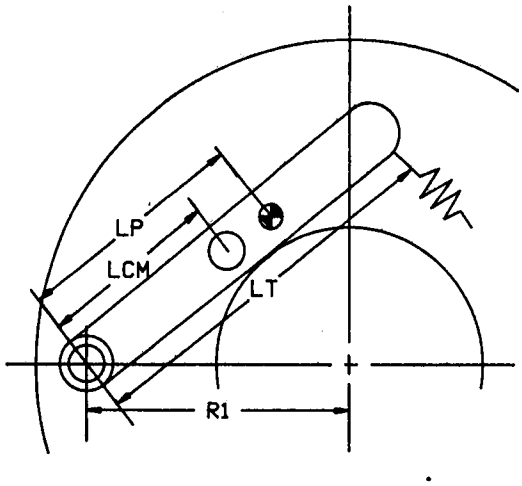


Figure 8. Illustration of the pivoting arm's geometrical variables.

3. The next variable was the distance from the pivot point to the center of mass (LCM). This would ultimately be decided by the shape of the arm. Therefore, knowing how the position of the center of mass changes the response is helpful when designing the pivoting arm. Varying the distance from pivot to centroid changes the moment arm of the centrifugal force. The combination of the mass and the vector

from pivot to centroid define the moment about the pivot point. The centrifugal moment produced at the specified design speed cannot be greater than that achieved by the preload of the spring. Consequently, this length is limited by the mass and spring preload combination.

4. Another variable was the distance from the pivot to the pin (LP). The moment arm of both the pin friction and torque reaction force is determined by this distance. Using a small distance would be useful to reduce the unwanted moments of the cam torque and, more significantly, the friction force at the pin. This radius also determines the displacement of the pin as it moves in the slot. This displacement is defined by:

$d = r * \Delta\theta$, where θ is the angle of rotation

r is the radius

In this case, a large displacement is desired to increase the accuracy of the rotation and decrease the slot angle. For this reason, a compromise had to be reached by using the minimum distance which would produce the desired displacement.

5. The final variable was the distance from the pivot to the point where the spring is attached (LT). The advantage here is to use the maximum possible distance to increase the moment arm of the spring. Again, the length of the arm is limited by the dimensions of the cam gear.

After studying computer output for a wide range of parameters, it was decided that the best workable design would have similar parameters to those listed below. The computer output illustrated the torque dependency and hysteresis associated with each different set of variables. The best design was defined by the set of parameters which produced the least torque dependency and hysteresis in the mechanism. The combinations were limited, however, by the preload and spring rate which could be achieved in the space available. The spring considerations are discussed further in the following section.

centrifugal weight--0.16 lb
spring rate , k --40 lb/in
preload, fo --28.2 lb
R1 --2.0 in
LP --.75 in
LCM --1.75 in
LT --3.0 in

The hysteresis observed when using the above set was considered too great for a successful design. It was decided to essentially eliminate the effect of friction by using rolling bearings. Such bearings have an average coefficient of friction of 0.001. Consequently, they eliminate

practically all sliding friction. Curves of the angular cam displacement verses cam speed for zero pin friction, variable pin friction, and variable cam torque with constant friction are given in Figures 9, 10 and 11. From the zero friction condition, it can be seen that, at constant speed, a 10 ft-lb increase in torque results in a maximum 29% change in displacement. The movement of the pivoting arm is not perfectly linear as can be seen from the figures. Estimating the motion as linear function gives the relationship between arm rotation and relative cam rotation as:

$$\underset{\text{CAM ANGLE (RAD)}}{\beta} = 0.058 \quad \underset{\text{ARM ANGLE (RAD)}}{\theta}$$

E. Spring Considerations and Analysis

A free-body diagram of the generic weight and pin assembly given in Figure 12 shows the forces acting on the link which define its motion.

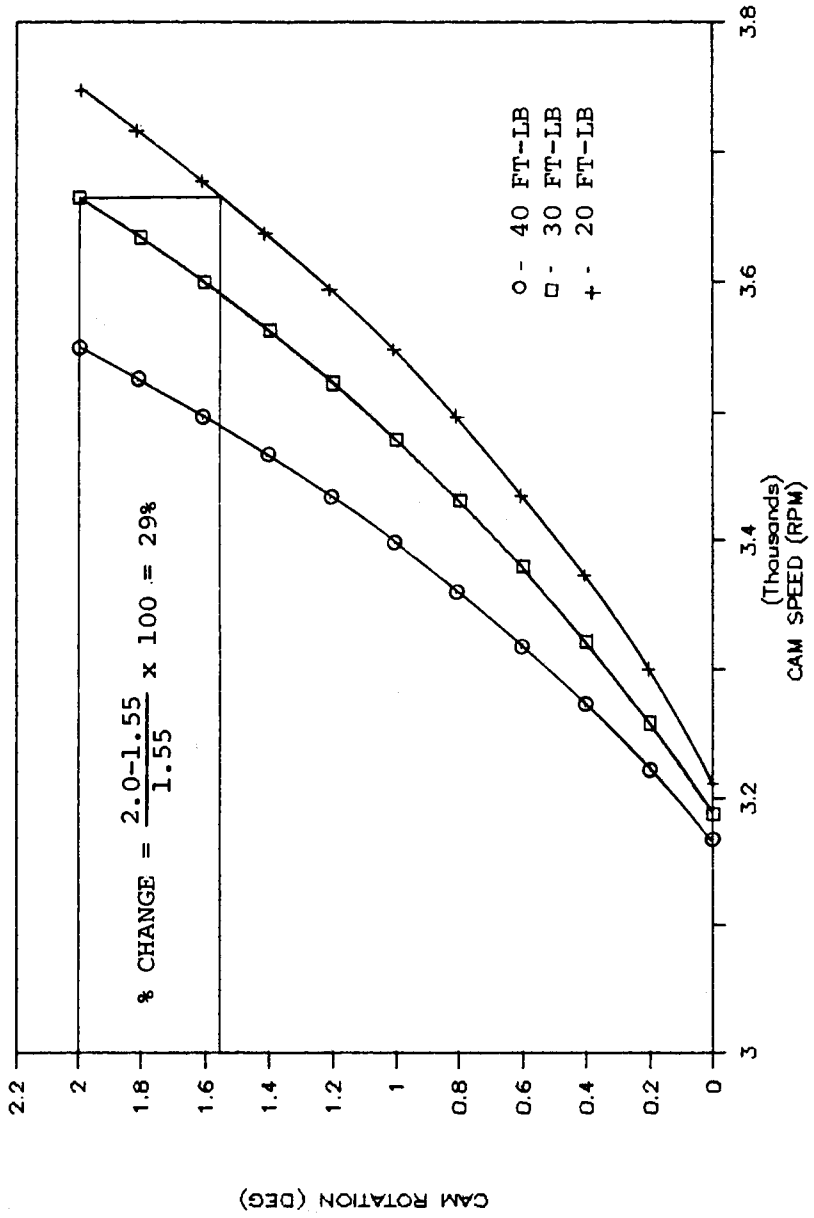


Figure 9. Theoretical cam speed vs. cam rotation curves for zero friction in the mechanism.

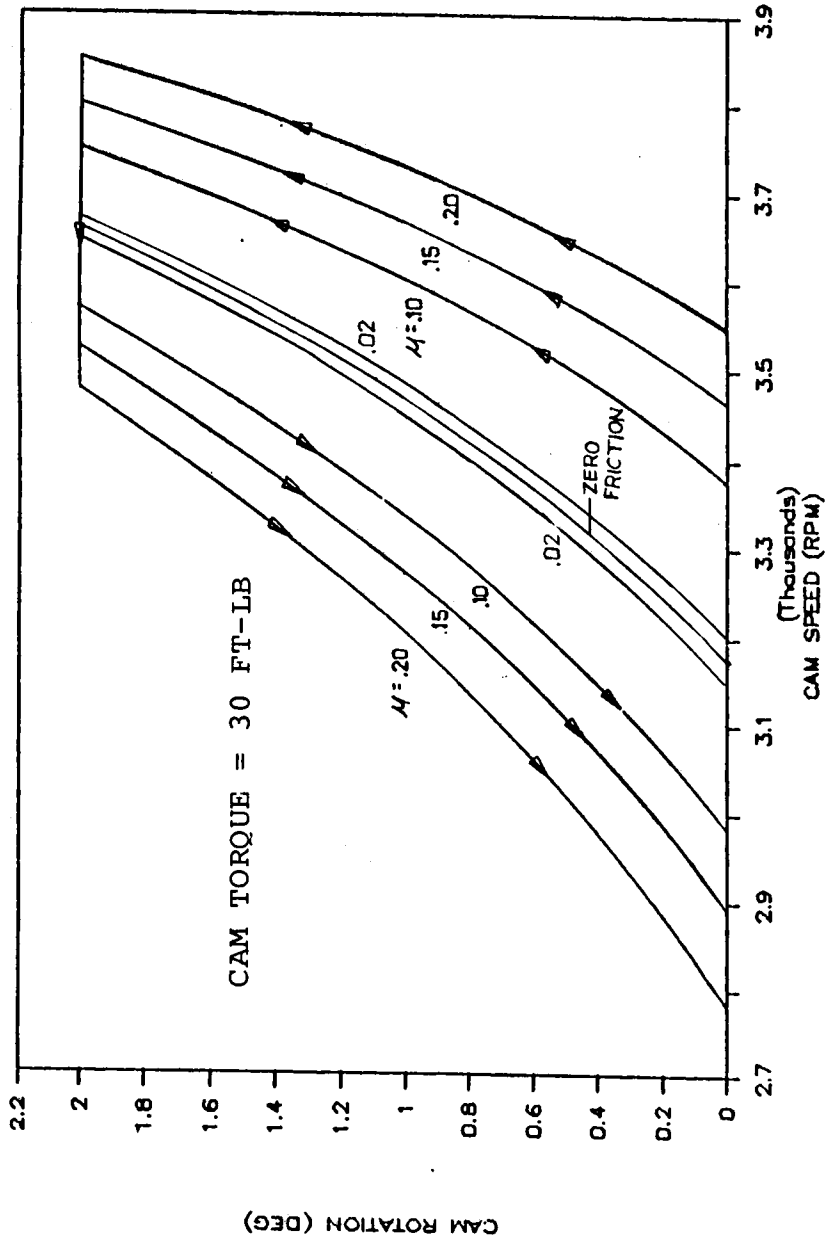


Figure 10. Theoretical cam speed vs. cam rotation curves for varying amounts of friction.

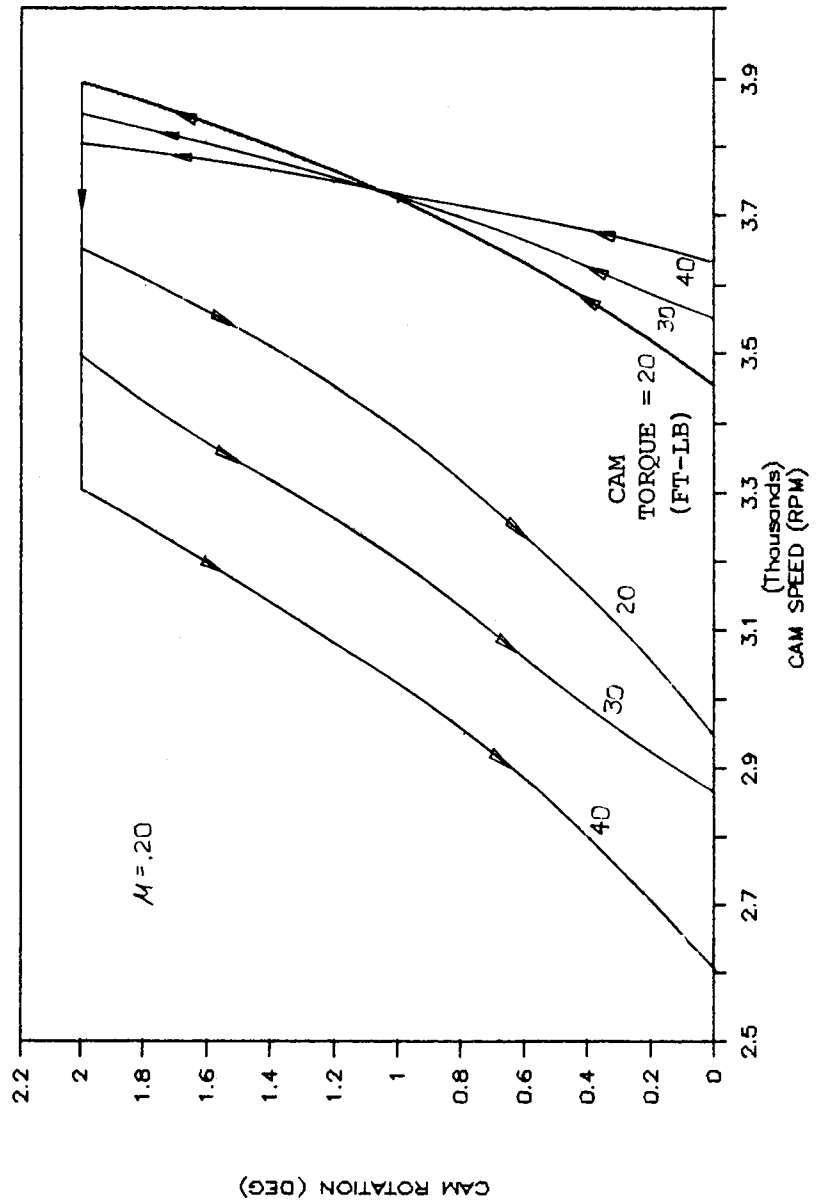


Figure 11. Theoretical cam speed vs. cam rotation curves for varying cam torque with constant friction in the mechanism.

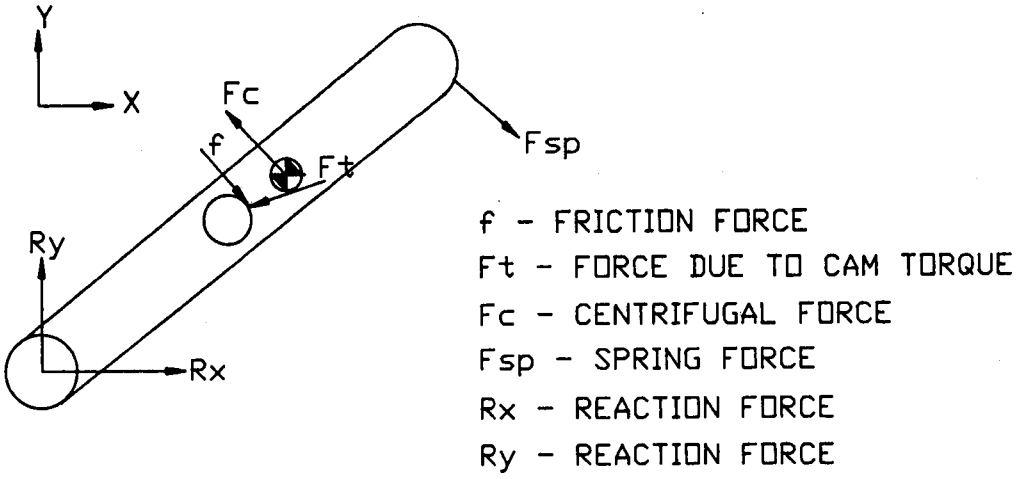


Figure 12. Free body diagram of the pivoting arm.

It is desired that the spring and centrifugal forces solely control the motion of the link. To achieve this result, the friction and torque reaction forces would have to be negligible relative to the spring and centrifugal forces. For this reason, large weights and stiff springs would yield the best design. High stiffness springs, however, cannot be deflected significantly because of high stresses. In this particular design, a large spring deflection is advantageous since it increases accuracy and decreases torque dependency. Also, a preload must be applied by the spring to restrict any motion of the weight until the specified cam speed has been reached. Therefore, a compromise between shear stress and deflection of the spring must be reached to prevent failure of the springs. Several types

of springs were considered to find the optimum stiffness/stress/deflection situation.

Before it was definitely decided to use pivoting weights, several types of springs were considered for the design. The deflections and dimensions of each type were limited by the dimensions of the cam timing gear, shown in Figure 13. Initial estimates of the required parameters were:

weight--0.1 lbs

spring constant--40 lb/in

spring deflection--0.5 in

maximum working depth--0.625 in

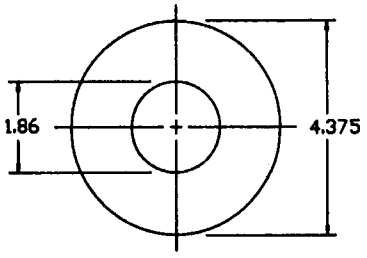


Figure 13. Inside gear dimensions.

1. Cantilever spring

Utilizing a cantilever spring was one method considered in the design. The analytical model, shown in Figure 14, shows the shear and moment diagram for the loading shown. Calculations of the maximum stress for a 40 lb/in effective spring rate beam revealed tensile stresses much greater than the yield strength of common steels (see Appendix A). For

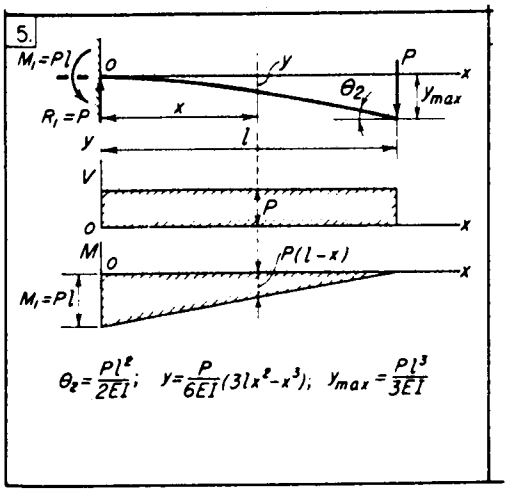


Figure 14. Cantilever beam analytical model.
Source: Spotts, M. F., Design of Machine Elements, sixth edition, 1985, p. 27.

this reason cantilever beams were no longer considered as a possibility (see Figure 15).

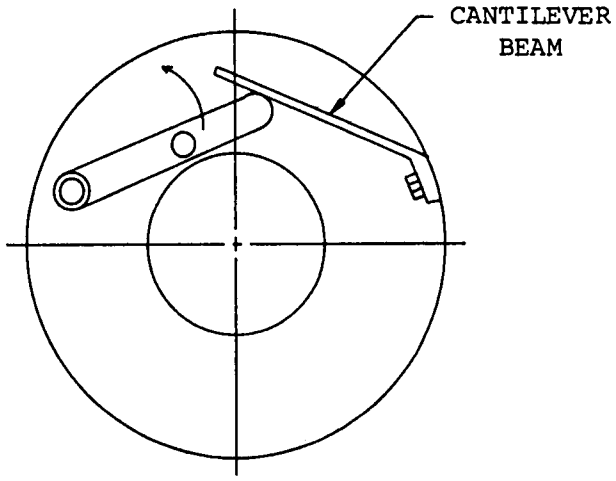


Figure 15. Configuration utilizing a cantilever beam.

2. Supported Straight Beams

Simply supported straight beams were another source considered to achieve the desired spring rate. The free-body diagram, shown in Figure 16, shows the combined bending and buckling loads for one configuration. The axial load increases the deflection and consequent stress of the beam over the simple bending case. The bending stress calculations, given in Appendix A, again produce a value (93,100 psi) too large to achieve an acceptable factor of safety. Used in the configuration shown below, the length and stability of the beam position could add further complications. For these reasons, straight beams were also dropped for consideration.

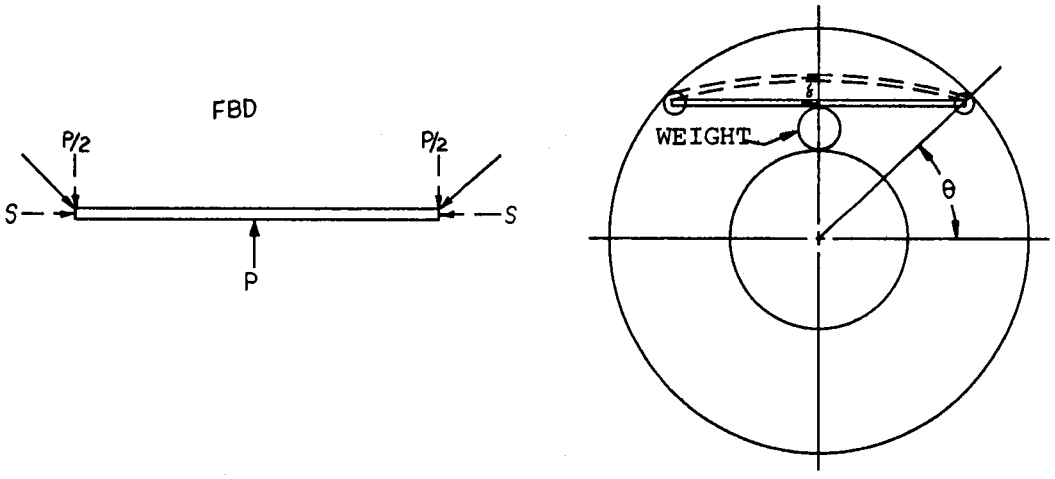


Figure 16. Configuration utilizing a straight beam.

3. Curved Beams

Curved beams were the next source considered to load the centifugal weights. Again the calculations produced stresses which would yield common steel (133,000 psi). Because of this, it was concluded that no type of rigid beam could be used to obtain an effective spring rate of 40 lb/in or greater. One possible configuration employing a curved beam is shown in Figure 17, along with the free-body diagram used for analysis.

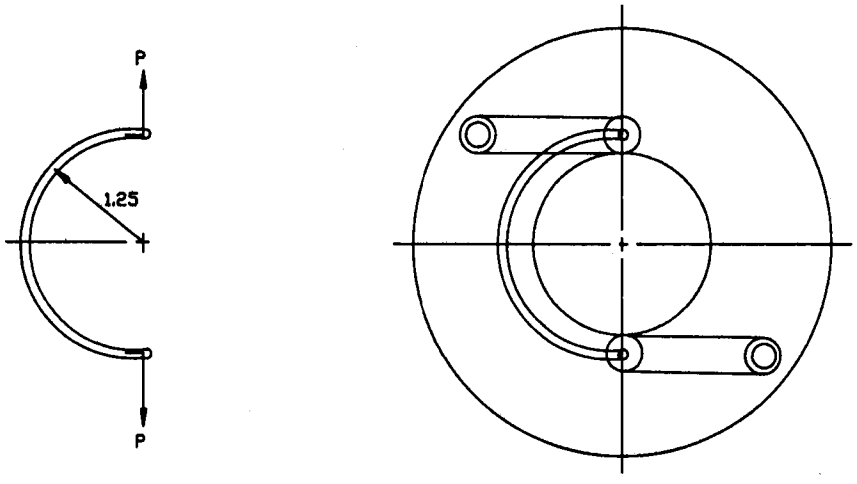


Figure 17. Configuration utilizing a curved beam.

4. Helical Coil Springs--(a) Compression, (b) Drawbar, (c) Extension

After eliminating the beams from consideration, the analysis moved to coil springs. Helical compression and

extension springs could be used in several different configurations. Therefore, they are better suited for this limited space problem. The general analysis of the helical spring is given below (see also Figure 18).

$$\text{Spring index, } C = 2R/d \tag{1}$$

$$\text{Stress factor (transverse shear), } K_s = 1 + \frac{.615}{C} \tag{2}$$

$$\text{Shear stress, } \tau = K_s \frac{16\ PR}{\pi d^3} \tag{3}$$

$$\text{Spring rate, } K = \frac{Gd}{8C^3N} \tag{4}$$

where G = shear modulus of elasticity,

N = number of active coils.

$$\text{Solid height, } L_s = N_t d \tag{5}$$

where N_t = total number of coils.

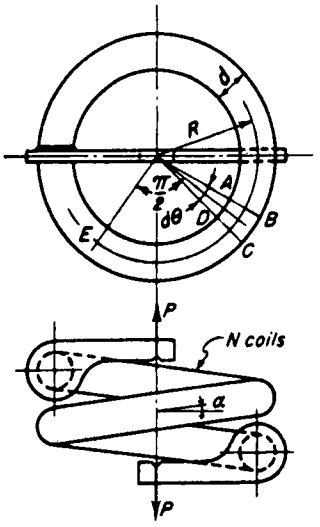


Figure 18. Helical spring formed from round wire.
Source: Spotts, M. F., Design of Machine Elements, sixth edition, 1985, p. 213.

Using the theoretical analysis, a computer program was developed for each form of the spring considered. Listings of each program are given in Appendix D. The computer programs were designed to vary wire diameter and number of coils in an attempt to find the lowest stressed spring which would satisfy the stiffness, preload, and length specifications.

a. Compression Springs

The analysis of compression springs revealed a dilemma between shear stress and solid height. Any spring meeting the required stiffness and diameter was either too long or exceeded an 80,000 psi limit for the shear stress when deflected. Fixing the spring into position was another

difficulty foreseen when using a compression spring. The two possible configurations utilizing compression springs, shown in Figure 19, were not thought to be workable designs. For these reasons, compression springs were quickly dropped from consideration in the design. Nested springs were also considered, but no usable combinations were found.

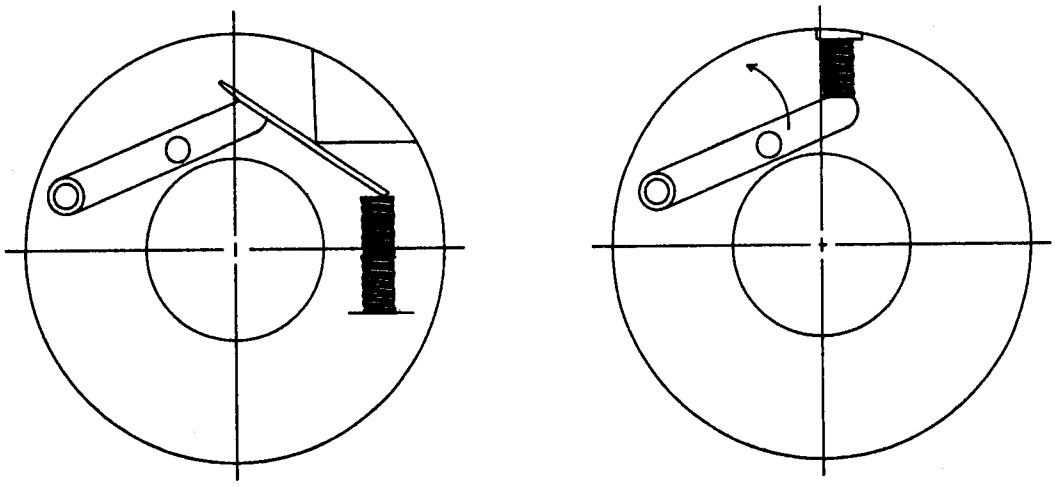


Figure 19. Possible compression spring applications.

b. Drawbar Springs

Drawbar springs are compression springs adapted to be used as extension springs by utilizing two hooks through the center of the spring as shown in Figure 20. The hooks are analogous to the end loops of the common extension spring, and are usually rotated 90° relative to each other. The advantage of such a configuration is the absence of the

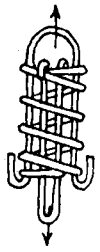


Figure 20. Drawbar spring.

usually large shear stress associated with the end loops of the extension spring. Addition equations for the behavior of the drawbar spring are given below. Using this analysis in addition to the general helical spring equations, the computer program was developed to produce many possibilities within the given constraints. Again it was discovered that every spring of acceptable stress would reach its solid height before the centifugal weight had pivoted the prescribed amount. Therefore, drawbar springs were also not used in the design.

Preload length, = 2.0 in

Free length, $L_f = 2.0 + f_0/K$ (6)

Solid length, $L_s = L_f = \frac{F_{max}}{K}$ (1.1) (7)

Max force, $F_{max} = f_0 + Ky_{max}$ (8)

Substitution of equations (5) and (8) into equation (7) yields

$$N_c d + \frac{0.1\ f_0}{K} = 2.0 - 1.1\ y \quad (9)$$

Substitution of equation (4) gives

$$N\ d + \frac{(0.1)f_0(8)D^3N_c}{d^4G} = 2.0 - 1.1\ y \quad (10)$$

Input f_0, d, D, y and solve for N_c, k, P, τ

c. Extension Springs

The analysis of extension springs is identical to that of compression springs except for the addition of end loop stress equations (see Figure 21). The bending stress at the loop is doubled compared to the shear stress in the spring. This is the major disadvantage associated with the extension spring. Some ways of reducing this stress do exist, including using reduced end coils of the spring as shown in Figure 22. This reduces the diameter of the end loop and, consequently, the moment produced by the load.

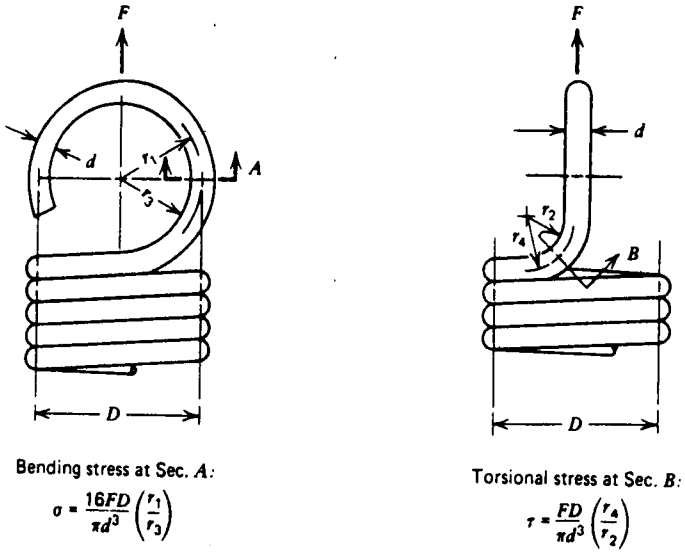


Figure 21. Conventional extension spring end loop.
Source: Juvinall, Robert C., Fundamentals of Machine Component Design, 1983, p. 376.



Figure 22. Reduced diameter end turns to decrease end loop stress.
Source: Juvinall, Robert C., Fundamentals of Machine Component Design, 1983, p. 376.

The advantages of the extension spring include, the simplicity of fixing the spring into position using the end loops and, more importantly, the ability to wind a preload into the spring at zero deflection. The recommended amount of shear stress caused by the prewound load is given by equation 11. Using a conservative shear stress limit and the corresponding preload, the computer program revealed the

significant advantage of the wound in preload. Several combinations of wire diameter and coil number yielded springs which would fit into the space and provide the required stiffness. For this reason, it was decided that helical extension springs would be the best choice for the design.

$$\tau_{INITIAL} = (0.4 \text{ to } 0.8) \frac{Sult}{C} \qquad (11)$$

5. Fatigue

After deciding on the type of spring, the fatigue factor had to be considered. Since it was desired to reduce the torque dependency of the mechanism to a minimum, the goal was to use the maximum stiffness spring while maintaining some factor of safety. Consequently, the spring could not be designed for infinite life. It was decided to design the spring for 10,000 cycles. The stress-life curve in Figure 23 shows how quickly the allowable stress decreases with the increased fatigue life. Also notice that a maximum shear stress any less than 50% of the ultimate strength would be safe at 10,000 cycles. This was the design criteria used for the maximum stress of the spring.

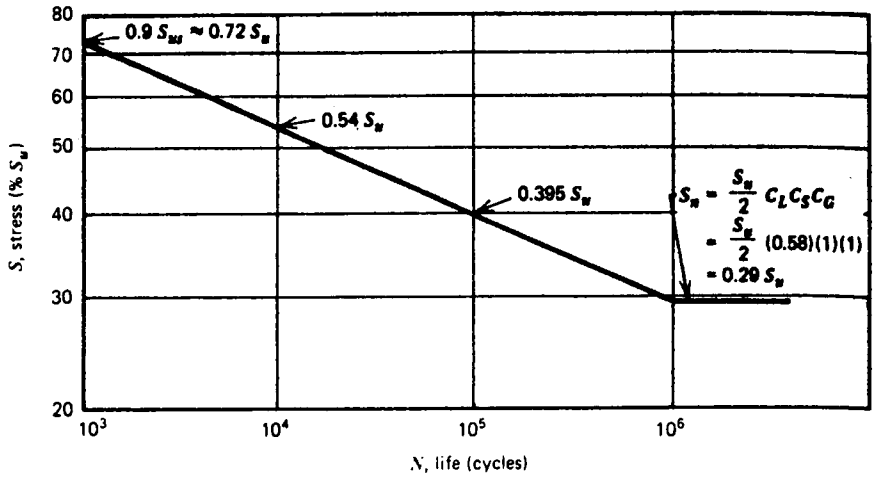


Figure 23. Estimated stress-life curve for round steel spring wire.
Source: Juvinall, Robert C., Fundamentals of Machine Component Design, 1983, p. 368.

CHAPTER 3

COMPONENT DESIGN

As in most machine design problems, each individual part cannot be designed independently. The components must be designed to work together while accomplishing the specified task. Although individual parts are discussed separately in this chapter, each was designed with the other components in mind. Each part, excluding the springs, is to be made of common low-carbon steel since no parts require unusual hardness or thermal properties.

A. Gear Preparation

The first step in the design of actual parts was to decide how much of the solid cam gear could be machined away to make room for the mechanism. The specific dimensions of an actual cast type, dual-row timing gear for a 350 cu. in. Chevrolet engine are given in Figure 24. The limit for the diameter to be cut out was set by the amount of gear covered by the timing chain. Adequate clearance must be specified to insure that the mechanism will not interfere with the chain. The depth of the cut was determined by the approximate cross-sectional area of the section between the holes

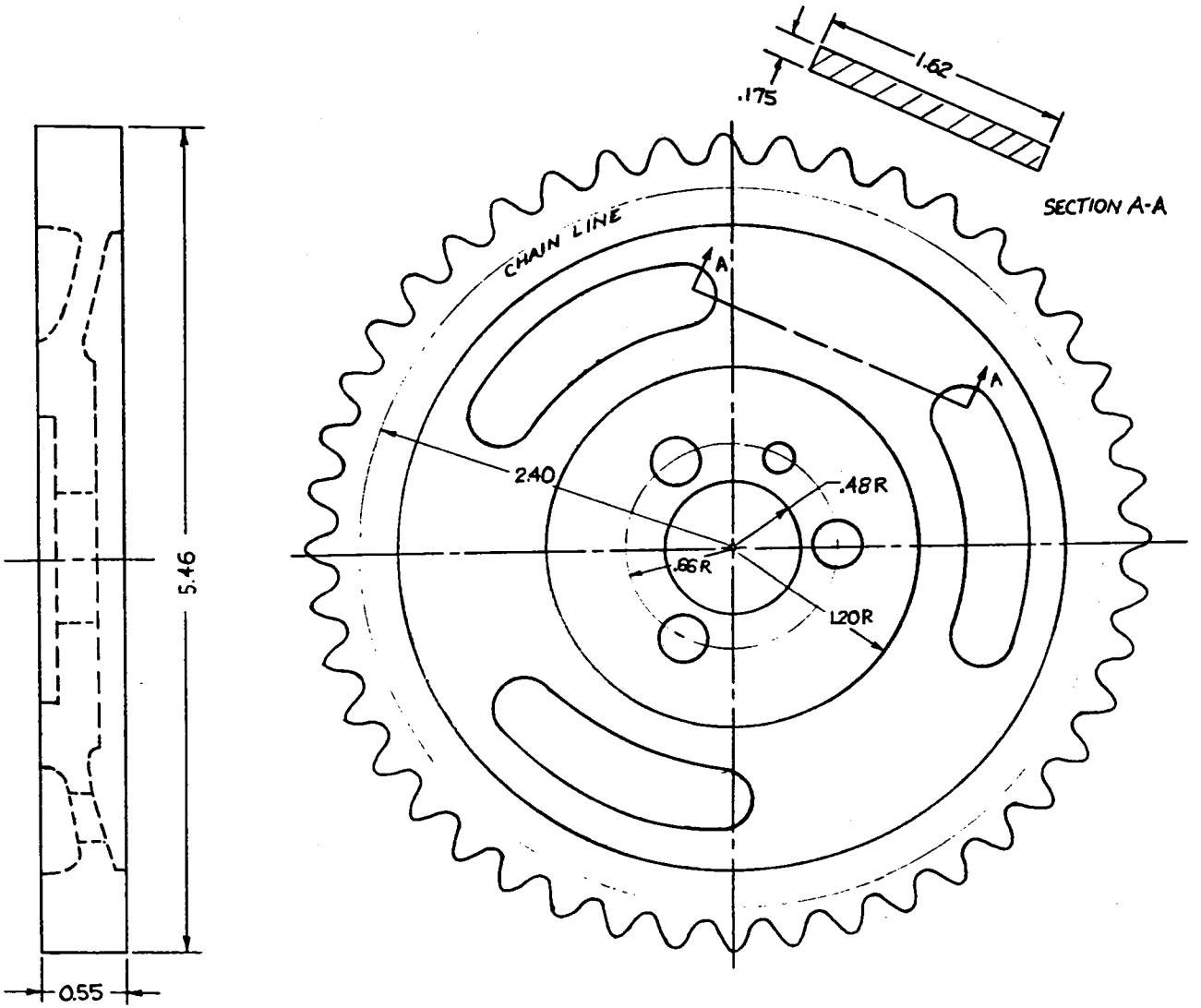


Figure 24. Basic dimensions of a stock timing gear for a 350 cu.in Chevrolet engine.

in the standard timing gear. This section is shown in Figure 24. If the three sections of this gear can support the torque on the gear, then a solid section of the same depth could also support the torque. Therefore, the depth of the cut was calculated by the total thickness minus the minimum thickness of the section. The thickness of the gear remaining also had to be large enough to attach the pivot pins securely. It was determined that this thickness would sufficiently support the pins. A hole through the center of the gear is determined by the diameter of the cam shaft end which was measured to be 1.86 inches. With the diameter, depth of cut, and the hole size determined, the cam gear design, shown in Figure 25, was complete.

B. Arm Design

The pivoting arm was designed to meet three specifications: (1) weight = 0.16 lb., (2) arm pivot angle = 0.3 radians and (3) springs to be attached. Ease of manufacturing was also a major consideration in the arm design. To conform to the weight specification, a shape was designed and the thickness varied to obtain the correct volume of steel. The maximum pivot angle is determined when the highest point of the arm contacts the outer gear surface. A trial and error graphical method was used to obtain the

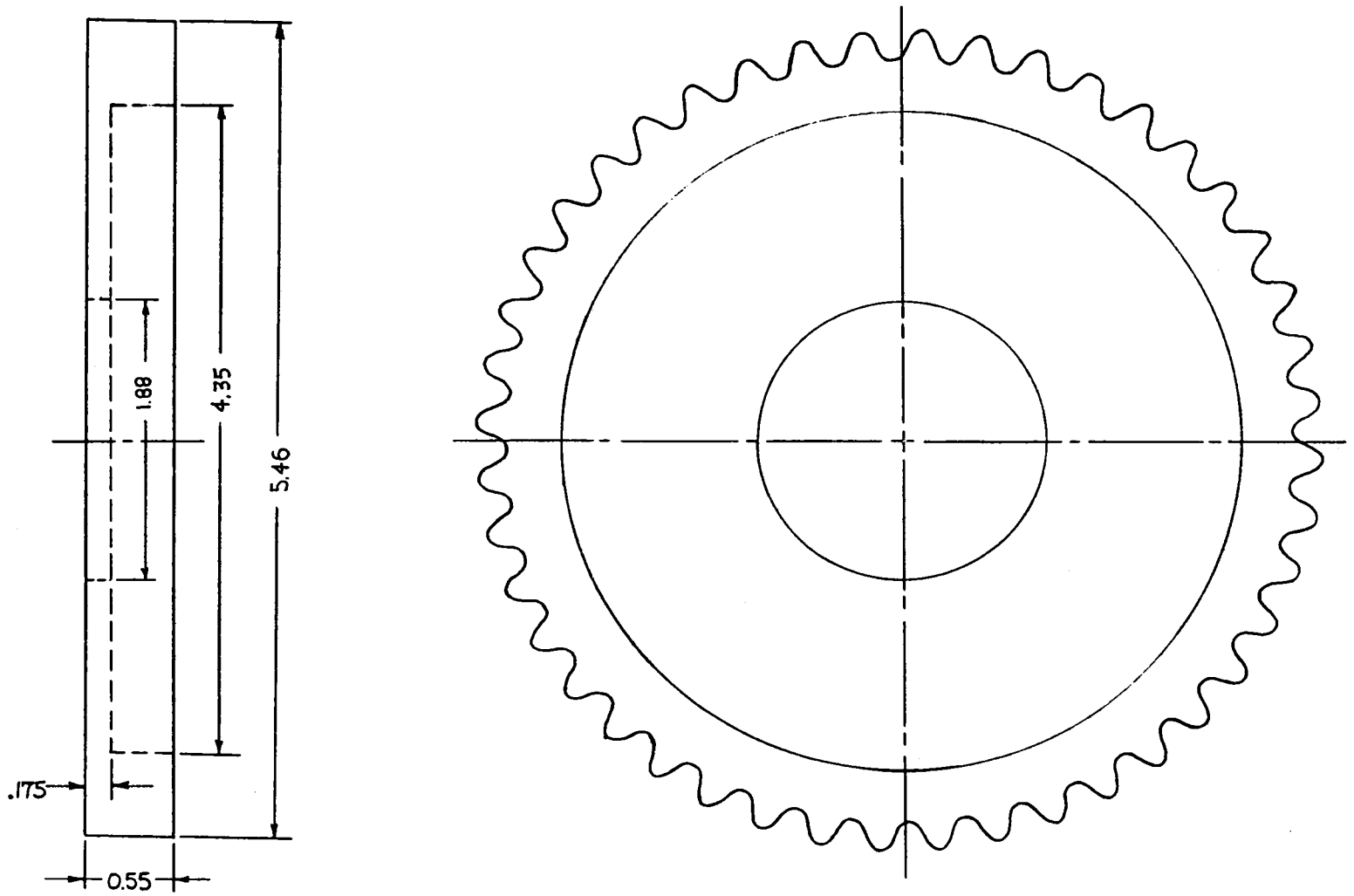


Figure 25. Cam timing gear detail drawing.

correct motion of this point. The optimum geometry described in the preceding chapter called for a pivot-spring distance of 3.0 inches. It was discovered an arm this long could not produce the specified rotation. Therefore, the arm was designed somewhat shorter. A spring post was specified at the end of the arm to attach the spring. This was the simplest method considered. Using a machine screw for the post would only require one additional tapped hole in the arm. Using as few curved surfaces as possible, the arm was designed for ease of fabrication. A detail drawing of the final arm design is given in Figure 26.

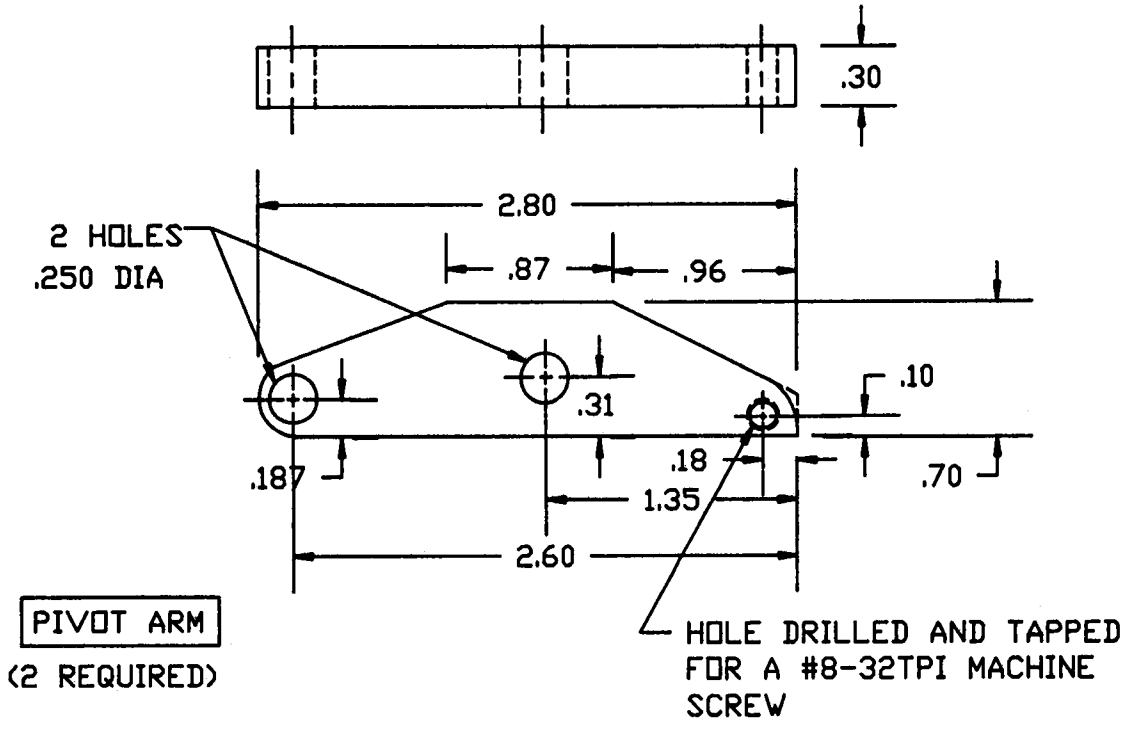
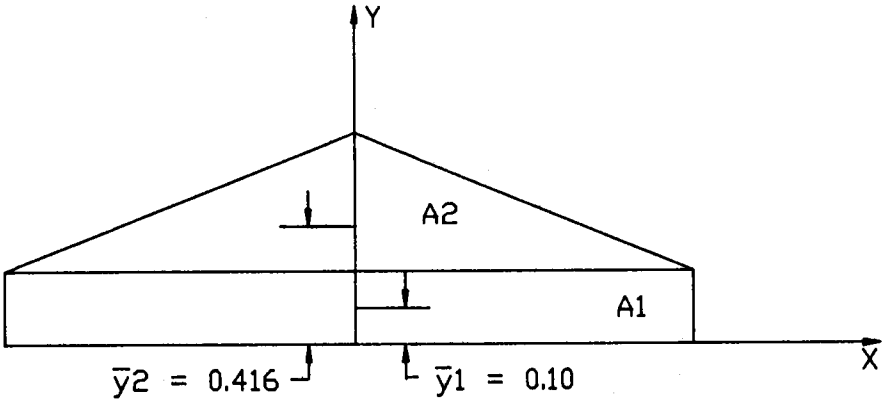


Figure 26. Pivot arm detail drawing.

The centroid of the arm was calculated for the purpose of defining the centrifugal force vector in the analysis. Estimating the section with no holes and squared on both ends, as in Figure 27, the vertical dimension, $\bar{y}$, was calculated using equation 12. Since the section is symmetric about the y-axis, the horizontal dimension, $\bar{x}$, equals zero.

$$\bar{y} = \frac{\sum_i A_i \bar{y}_i}{\sum_i A_i} \qquad (12)$$



	Area, in^2	$\bar{y}$1	Aiyi, in^3
A1	(.2)(2.8)=0.56	0.10	.056
A2	(.65)(2.8)=1.82	0.416	.757
ΣAi	2.38		.813

$\bar{y}$ = .813/2.38
= .34 in

Figure 27. Centroid location calculation.

C. Spacer and Drive Plate Design

The spacer was the easiest of all the parts to design since all of the dimensions were predefined except for the length. One end of the spacer had to fit on the end of the cam shaft. Therefore, both the position and diameter of the dowel pin and bolt holes were already specified. The other end of the spacer required only a center and another dowel pin to fix the position of the drive plate. The position of the dowel pin was arbitrary as long as it did not interfere with the bolt holes. The length of the spacer was determined such that it passed through the thickness of the gear and passed the springs as shown in the Figure 28. This insures no contact between the springs and drive plate. The diameter of the spacer must be slightly smaller than the hole in the gear to allow relative rotation. The clearance must be kept to a minimum, however, to maintain alignment and avoid "slop" in the mechanism.

The difficult part in designing the drive plate was determining the slot angle. A graphical analysis, shown in Figure 29, was completed after the bearing position and size had been specified. The angle of the slot had to produce the specified 2° of relative cam rotation. The slots were extended to the perimeter of the plate to simplify fabrication. Special care should be taken to insure symmetry of

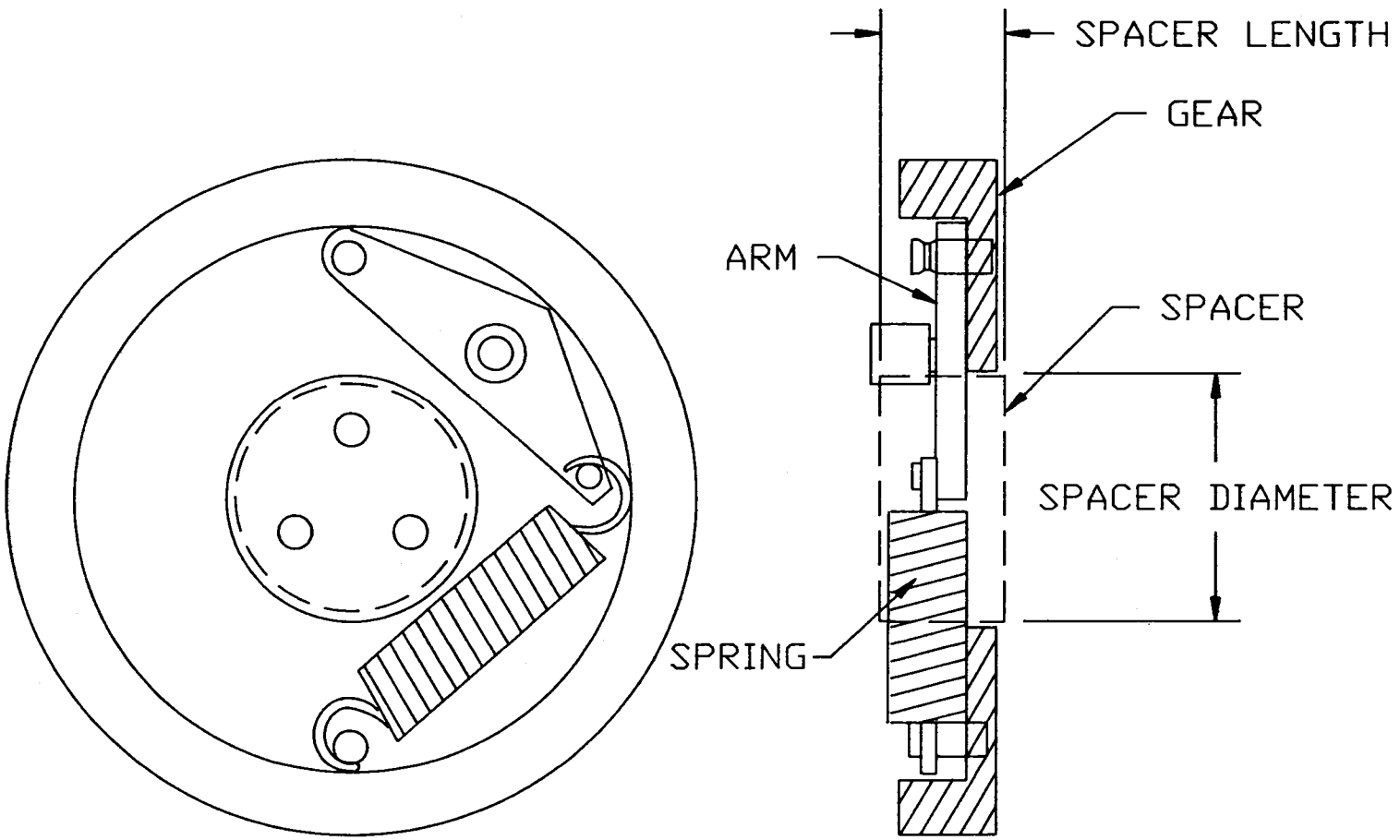


Figure 28. Spacer orientation within the mechanism.

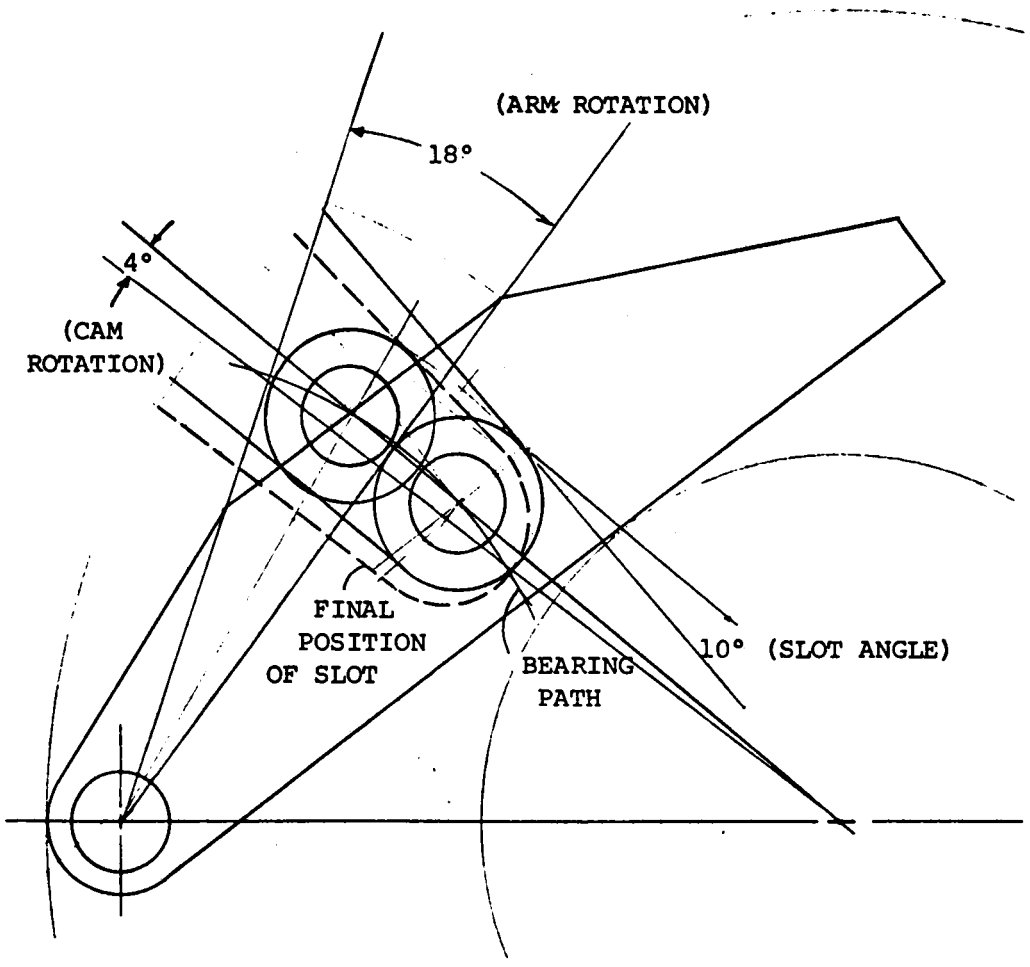


Figure 29. Graphical determination of the cam rotation for a given slot angle.

the slots. Loss of symmetry in the mechanism can cause binding because the arms must rotate simultaneously. The bolt holes in the plate matched those of the spacer. See Figures 30 and 31 for the detailed drawings of the drive plate and spacer.

D. Fasteners

The pivot pin and bearing shaft are both short steel rods which are knurled on one end and pressed into the gear and arm, respectively. The pivot pin about which the arm rotates has a groove cut in the opposite end. This end serves as a spring post for one end loop of the spring. The bearing shaft also has a groove cut in one end. A small snap ring is placed in this groove to hold the bearing in place. The only other fasteners are the three bolts which fix the gear to the cam shaft. These must be slightly longer than the original bolts of the standard timing gear (2" long, 5/16"-18 TPI). (See Figure 32.)

E. Bearing Selection

The first consideration in selecting a bearing was the size. It was desired to use the smallest diameter bearing which would carry the load. Needle bearings were considered

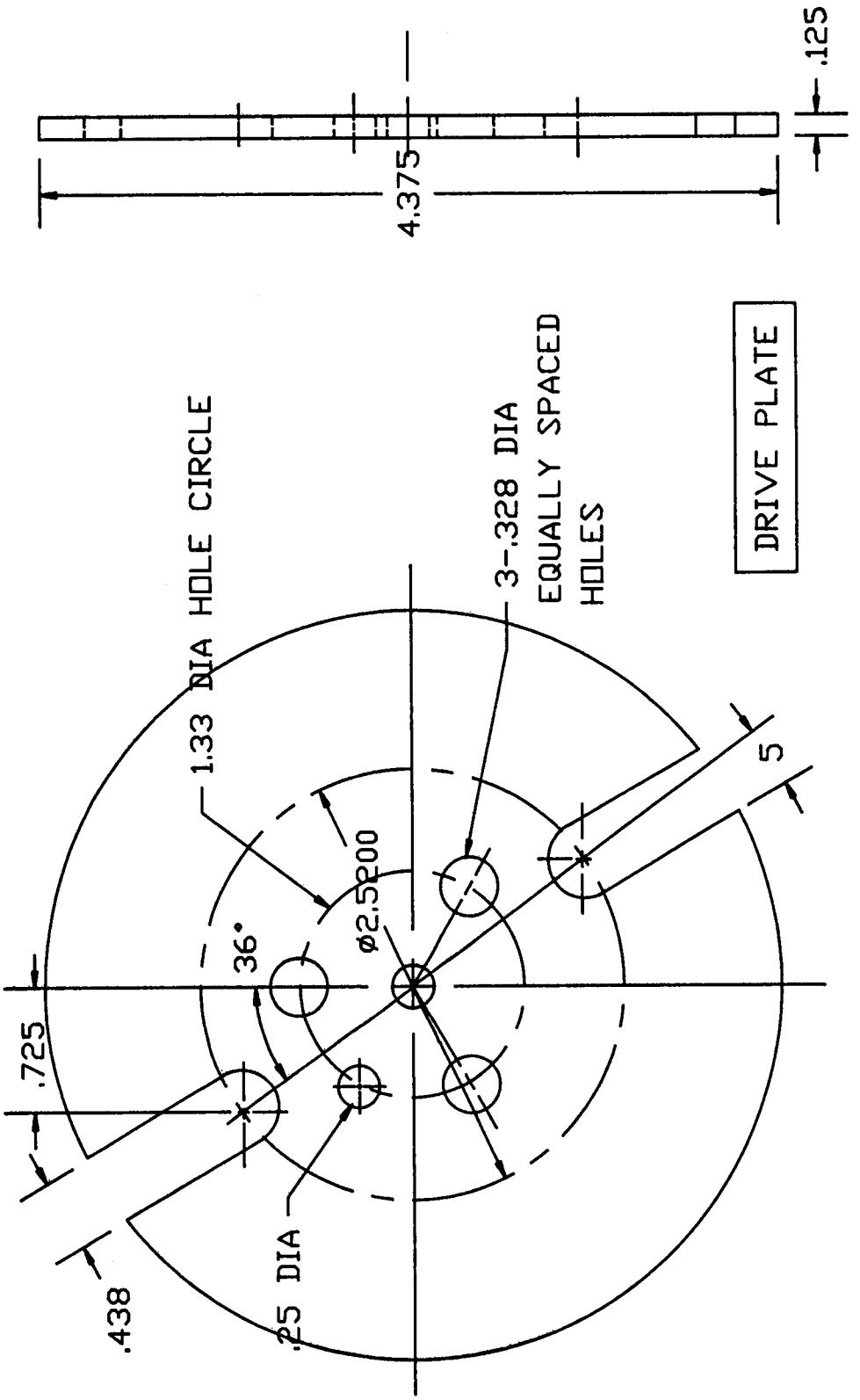


Figure 30. Drive plate detail drawing.

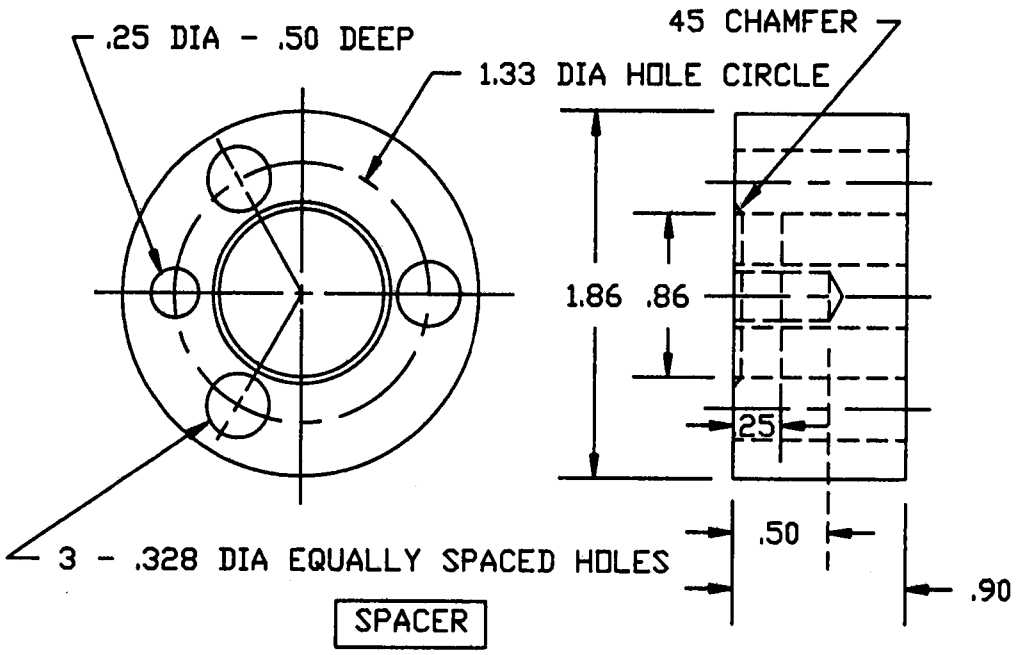


Figure 31. Spacer detail drawing.

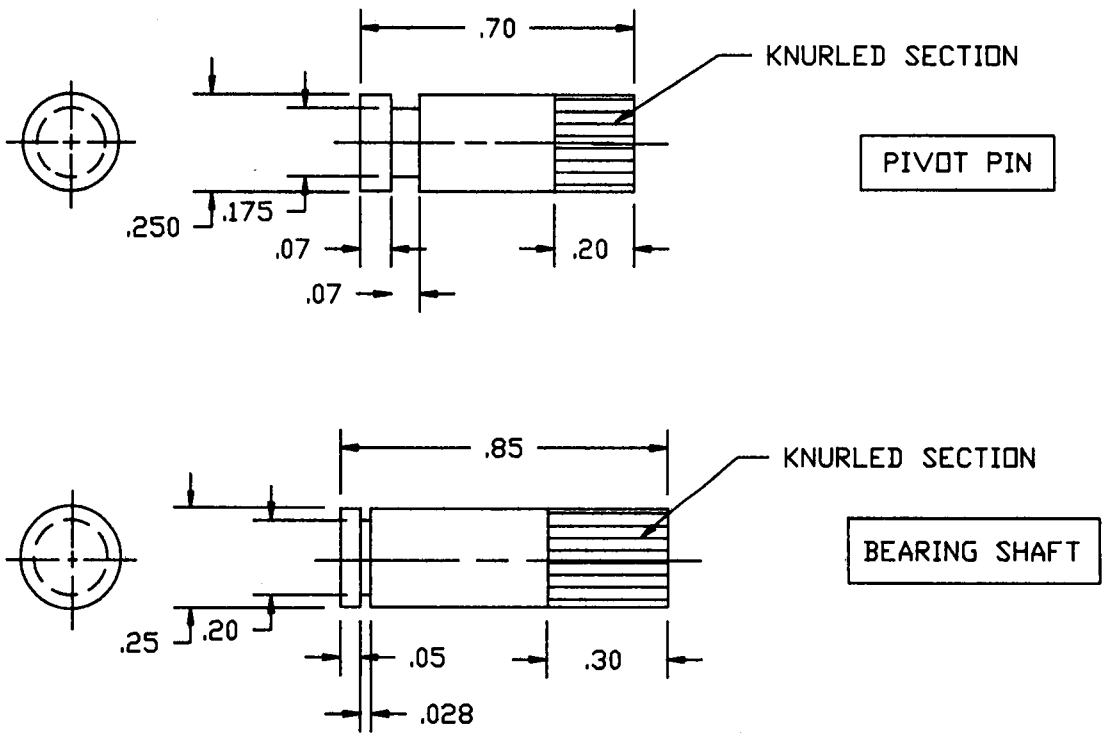


Figure 32. Pivot pin and bearing shaft detail drawings.

first because they have the smallest outer diameter to inner diameter ratio. After some research, it was discovered that needle bearings have a greater load capacity for any given shaft size than any other roller bearing. This results from the large contact area because more rollers are used. With the greater contact area, the needle bearings had lower speed capability than other bearings. For this application, however, speed was not a factor and needle bearings became the obvious choice. The particular bearing chosen was 0.25 in. ID, 0.4375 in. OD and 0.4375 in. long.

F. Spring Specifications

Spring rate--40 lb/in
Wire diameter--no.12 gage , 0.1055 in
Number of active coils--12.25
Loop diameter--0.45 in
Nominal spring diameter--0.520 in
Spring index--4.95
Free length(inside end loops)--2.186 in
28.2 lb Preload length--2.40 in
20 lb wound in preload
Maximum deflection--.944 in
Max stress(bending)--160,000 psi
Max stress(shear)--73,000 psi

Material--Valve Spring ASTM A230

Recommended Tolerances: free length--.060 in

coil diameter--.007 in

wire diameter--.0010 in

G. Assembly

The assembly of the mechanism is a relatively simple procedure outlined by the steps below. The only difficult process foreseen is the stretching and placement of the springs. Table 1 lists all of the parts required for the completed mechanism. The complete assembly view is given in Figure 33.

1. Press the knurled pivot pins and bearing shafts into the cam gear and arms, respectively.

2. Place the arms on the pivot pins and check for free rotation.

3. Insert the spacer into the hole through the cam gear.

4. Insert the machine screw spring posts into both arms.

5. Stretch and place the extension springs into position on the posts.

6. Place the bearings on their respective shafts and secure with the snap rings.

TABLE 1. PARTS LIST

PART NO.	QUANTITY	PART NAME	STOCK MATERIAL/SPEC.
1	1	CAM GEAR	5.5 in. ROUND STOCK
2	2	PIVOT PIN	.25 in. ROUND BAR
3	2	PIVOT ARM	.50 in. FLAT PLATE
4	2	MACHINE SCREW	#8,32TPI,SOCKET HEAD
5	2	SPRINGS	SEE PAGE X
6	2	BEARING SHAFT	.25 in. ROUND BAR
7	2	BEARING	NEEDLE,.25ID,.4375OD
8	2	RETAINING RING	.25 in. SHAFT SIZE
9	1	SPACER	1.875 in. ROUND STOCK
10	1	DOW PIN	.25 in. ROLL PIN
11	1	DRIVE PLATE	4.5 in. ROUND STOCK
12	3	GEAR BOLTS	5/16"-18UNC-2A
TOTAL	21 PARTS		

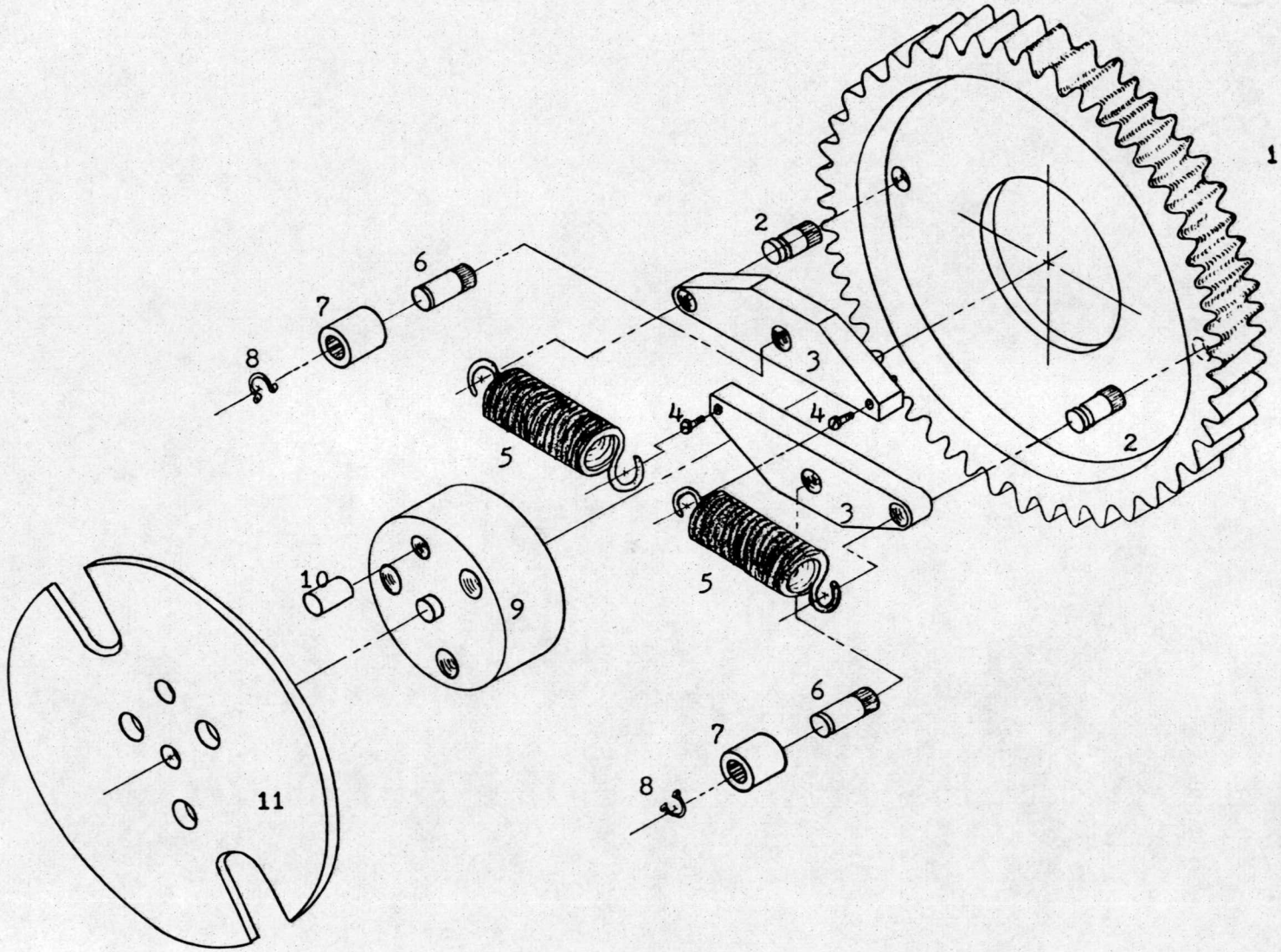


Figure 33. Assembly view of the final cam retarder design.

7. Align the drive plate on the bearings and pin of the spacer.

8. Bolt the entire assembly to the cam shaft with the three hex head screws.

CHAPTER 4

PROTOTYPE DESIGN

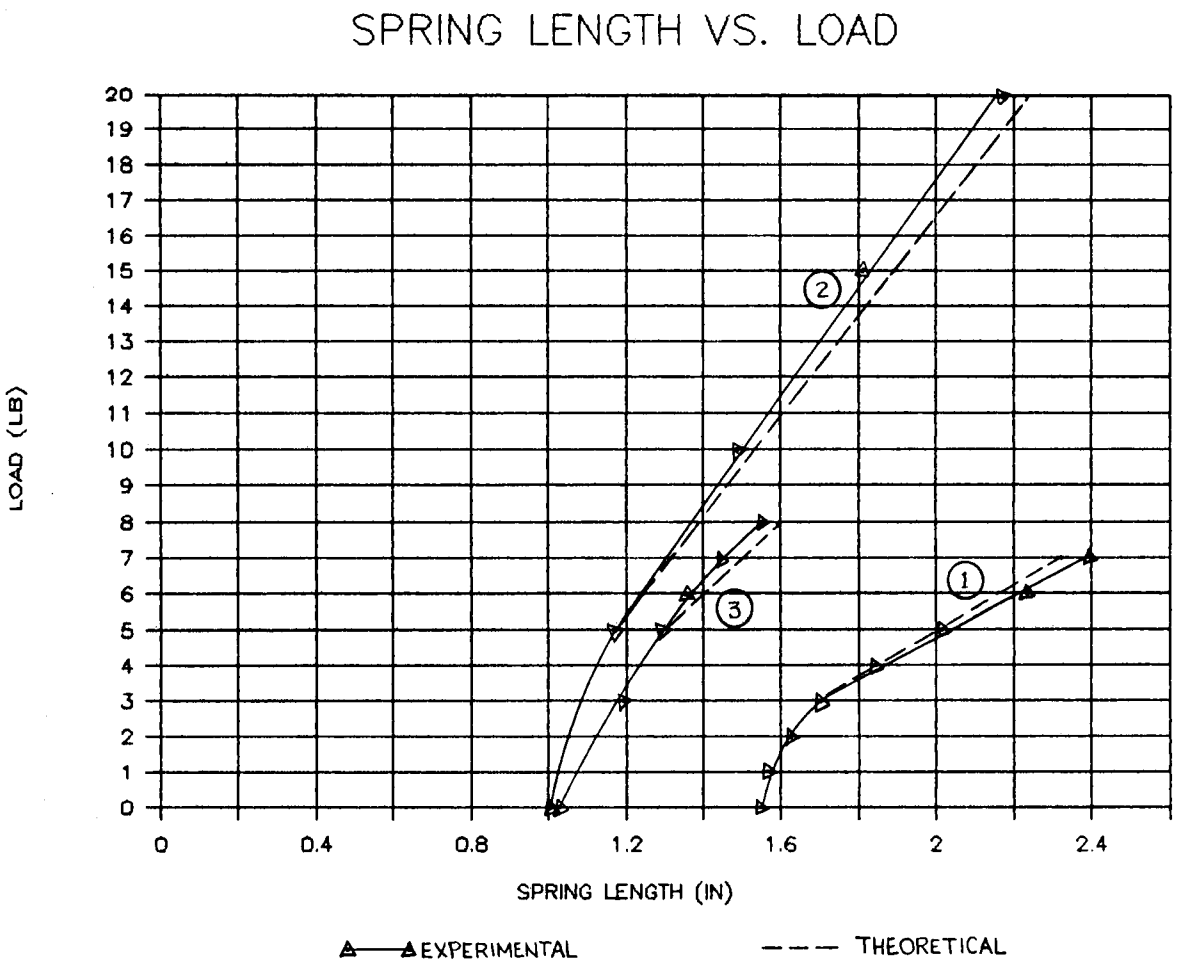
A prototype cam retarding mechanism was developed for testing purposes. Several changes were made in the design for various reasons. Expense and machine shop capabilities limited the prototype fabrication to a stock cam timing gear. For this reason a plate was designed to mount on the gear. This additional plate provided the surface needed to attach the pivoting arms. As mentioned earlier, it was intended to operate the prototype at lower speeds. Therefore, the springs employed were much more flexible than those specified in the final design. The flexible springs produced only a small preload on the arm and , consequently, less centrifugal force was required to begin rotation of the arm. The stiffness of the three springs available for testing of the prototype was determined both experimentally and analytically. Table 2 lists both the dimensions and calculated spring parameters. The experimental test data is shown in Table 3. A comparison of the two results is charted in Figure 34.

TABLE 2. SPRING PARAMETERS

SPRING	1	2	3
D	.333	.474	.325
d	.047	.063	.047
c	7.08	7.52	6.91
K	5.93	14.2	9.30

TABLE 3. SPRING TEST DATA

SPRING	LOAD(LB)	LENGTH(IN)
1	0	1.55
	1	1.57
	2	1.62
	3	1.70
	4	1.85
	5	2.05
	6	2.25
	7	2.40
2	0	1.00
	5	1.17
	10	1.48
	15	1.81
	20	2.17
3	0	1.08
	3	1.20
	5	1.28
	6	1.36
	7	1.45
	8	1.55



$$K_1 = \frac{7.0-3.0}{2.4-1.7} = 5.7 \text{ lb/in}$$

$$K_2 = \frac{20.0-5.0}{2.17-1.17} = 15.0 \text{ lb/in}$$

$$K_3 = \frac{8.0-5.0}{1.55-1.28} = 11.1 \text{ lb/in}$$

Figure 34. Experimental spring rate curves.

The weight of the arms was slightly decreased to reduce the preload requirement of the springs also. The angle of the slots in the drive plate was increased to provide approximately 5° of relative rotation. The purpose of this change was to insure easy detection of the rotation during testing of the prototype. Another minor variation was the bearing keeper. A small washer and screw were used to retain the bearing instead of the snap ring specified. See Figures 35-40 for individual prototype parts and the completed assembly. Figure 41 compares the cam retarding mechanism to a standard timing gear.

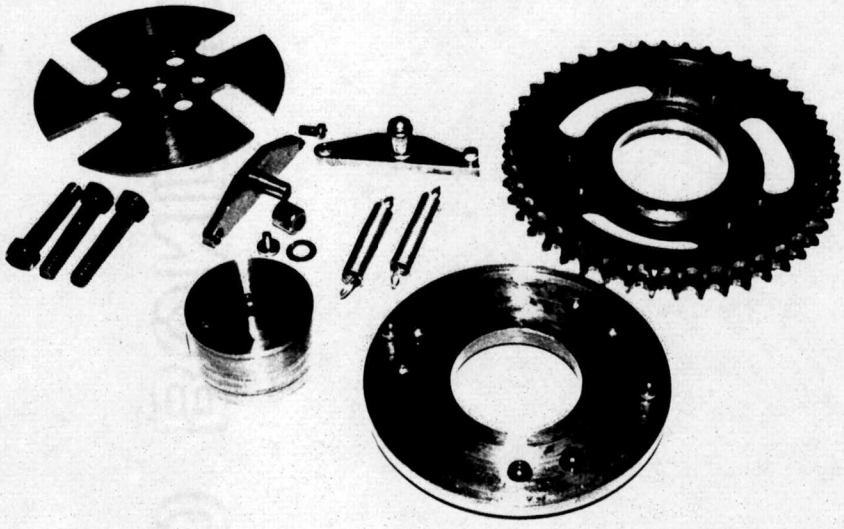


Figure 35. Complete parts display of prototype mechanism.

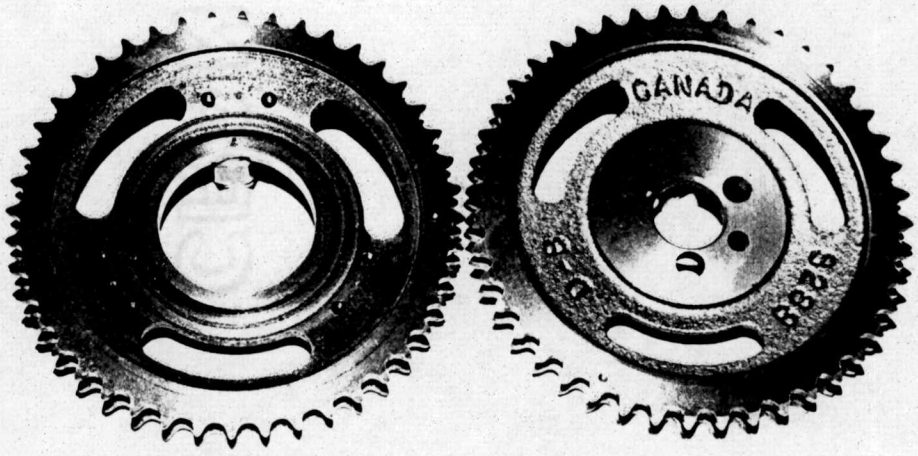


Figure 36. Stock timing gear before (right) and after (left) machining.

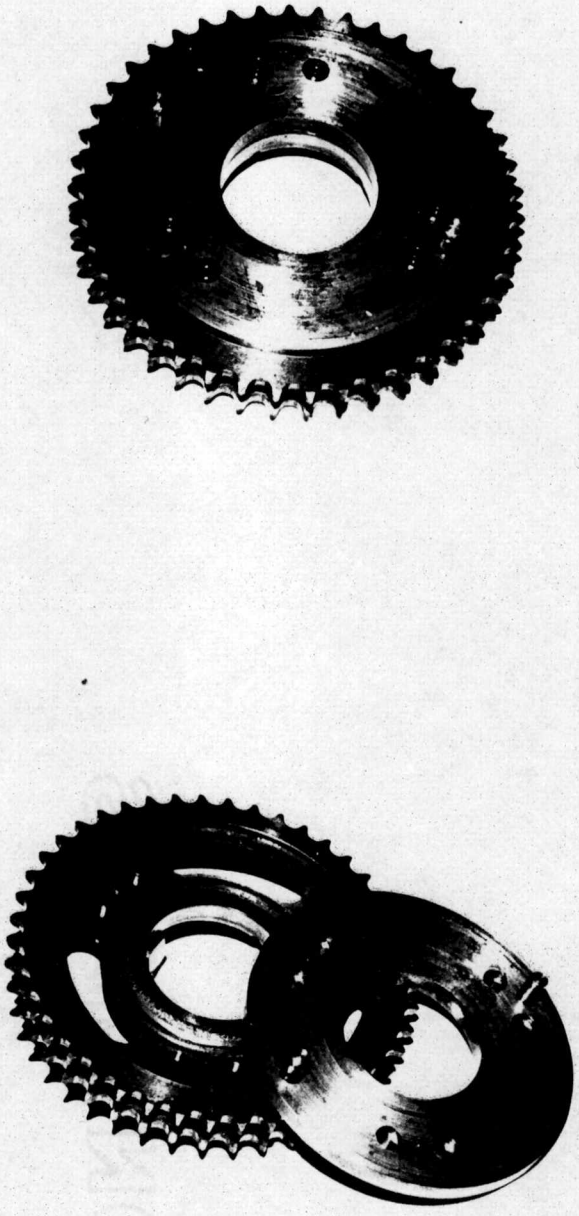


Figure 37. Gear and mounting plate assembly.



Figure 38. Spacer back side (above) and front view.

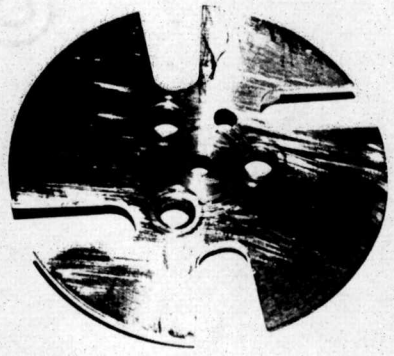


Figure 39. Drive plate.

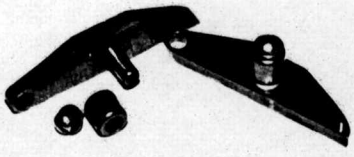


Figure 40. Pivot arm with and without bearing attached.

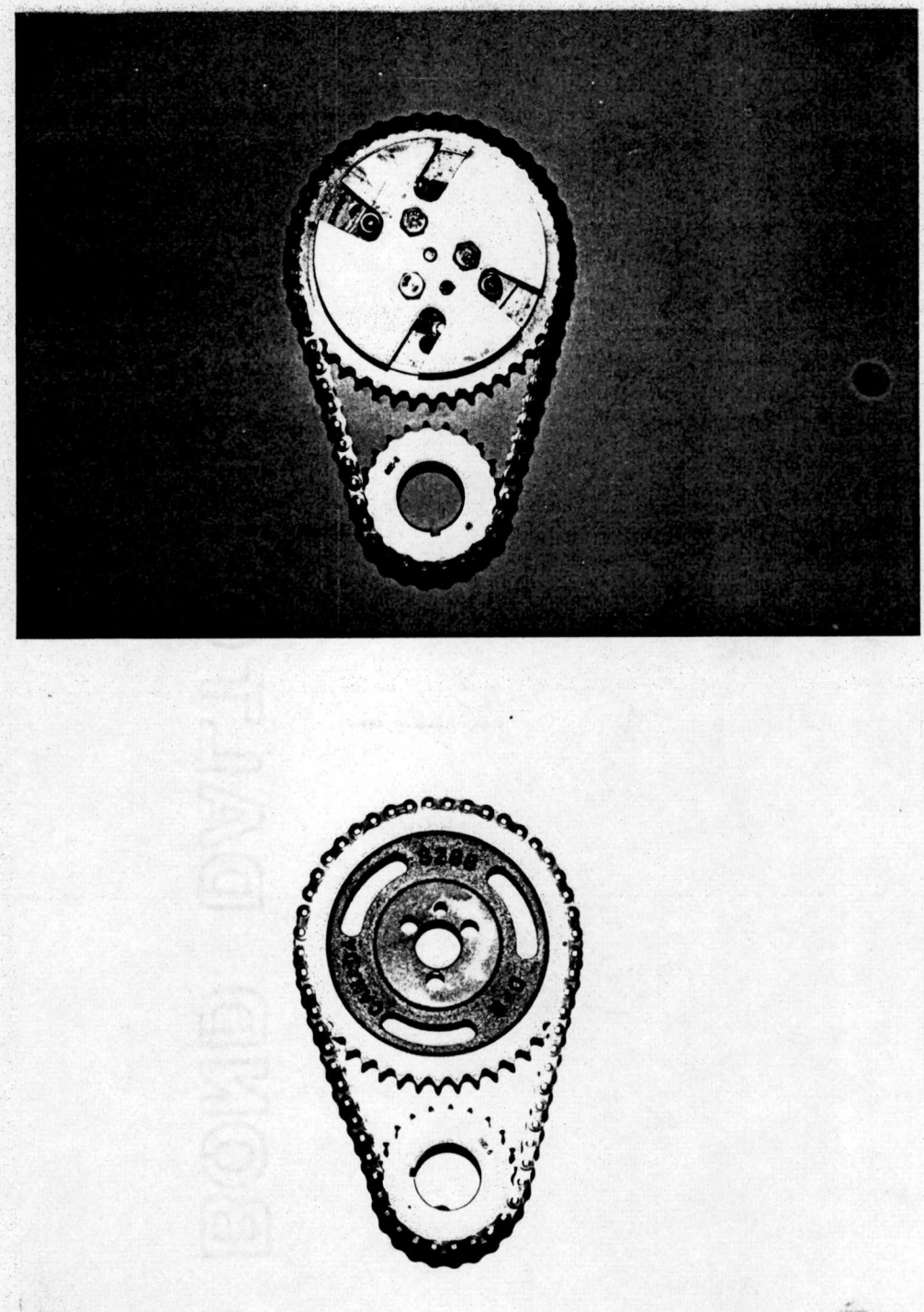


Figure 41. Assembled cam retarder timing configuration (above) and standard timing gear (below).

CHAPTER 5

PROTOTYPE TESTING

A. Experimental Set-up

The planned experimental apparatus required three major parts: (1) a dynamometer capable of producing the desired speeds, (2) a stock Chevrolet 350 cu.in. engine and (3) a drive train to couple the two together. The dynamometer required was currently set up with a Ford straight six cylinder engine. The Ford engine was removed to accommodate the new test engine. A used Chevrolet engine was obtained for the experiment. This engine was cleaned and rebuilt to reduce the chance of any part failures during testing. Carburetor, exhaust outlets, fuel pump, and other systems involved in actual firing of the engine were not required. Therefore, only the block, pistons, cam, heads, intake, and a distributor to drive the oil pump were needed for the experiment. It was quickly discovered that the space under the stock timing cover was much less than originally thought. Consequently, the cam retarding mechanism would not fit under the cover. To eliminate this problem, a hole was cut in the stock cover and the special Plexiglass cover, shown in Figure 42, was fabricated to enclose the mechanism.

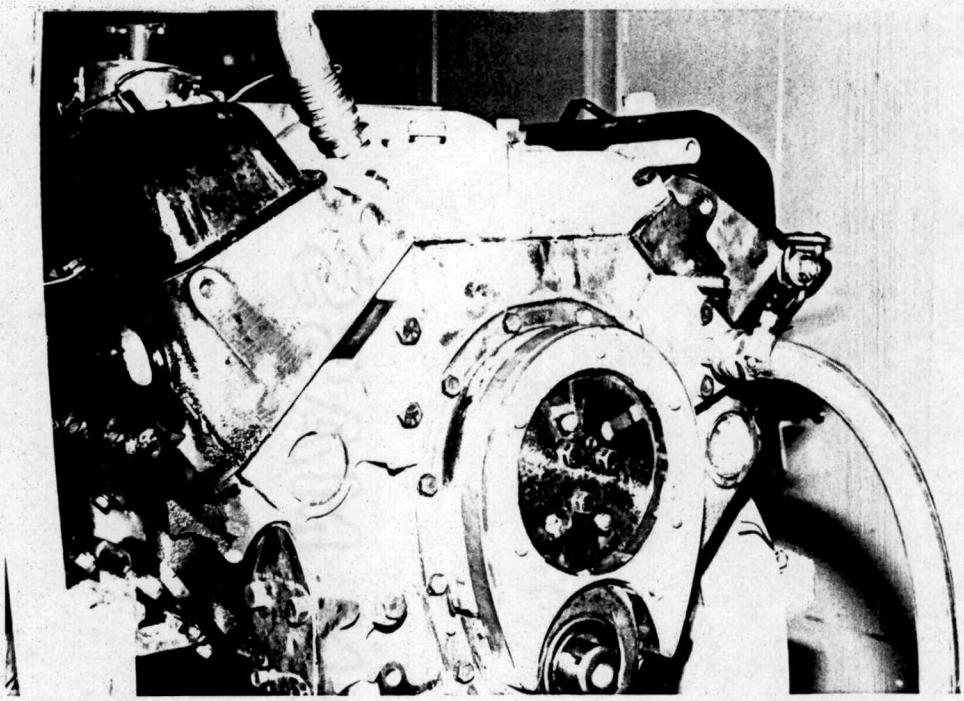


Figure 42. Fabricated plexiglass timing cover mounted on the test engine.

It was desired to have a means of uncoupling the system without major difficulty. Utilizing some type of clutch or transmission would accomplish this goal, but due to the unavailability and added expense of a Chevrolet transmission and clutch, the idea of obtaining one was dismissed. Therefore, it was decided to implement the transmission from the Ford engine if possible. An adapter plate to mount the transmission to the bell housing and a direct drive flange to replace the clutch were designed and built for the coupling device. Employing this system, the experimental

apparatus could be easily uncoupled by putting the transmission in neutral. The actual test set-up is shown in Figure 43.

B. Testing Procedure

One of the slots in the drive plate was marked in sections representing the percentage of full rotation of the arm. The full range was divided into eight sections; 12.5%, 25.0%, 37.5%, etc. (Figure 44).

The mechanism motion was observed using a stroboscope flashing at the corresponding cam speed. The dynamometer speed was increased until the bearing reached each of these marks. The cam speed was recorded at each position. The speed was then decreased and recorded at each mark as the bearing moved down the slot. This allowed the observer to identify any hysteresis of the motion.

C. Experimental Results and Comparison

The original slots cut in the drive plate were approximately 30° relative to a radius from the center. This resulted in a large moment arm for the torque reaction force (Figure 45).

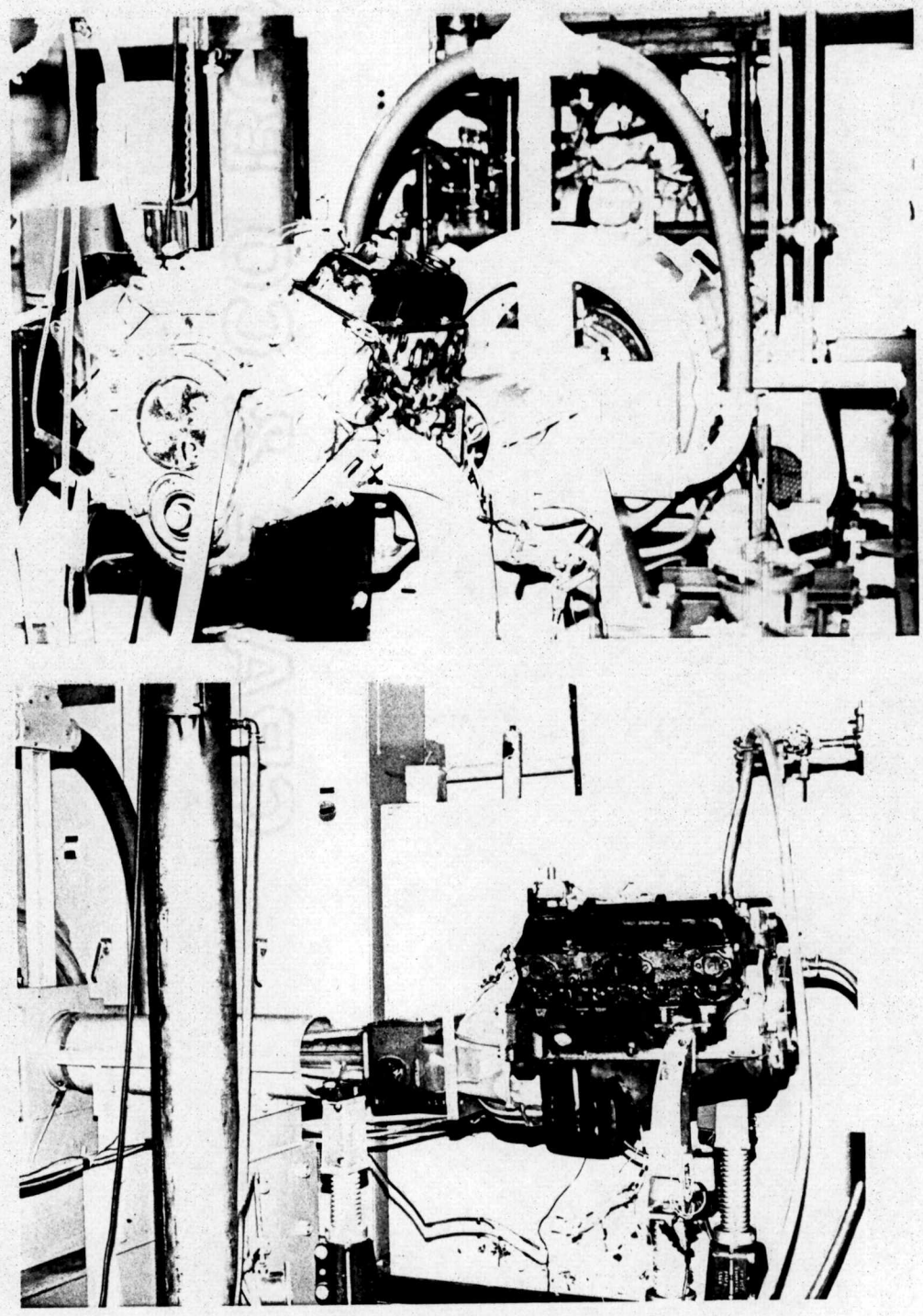


Figure 43. Test set-up. Notice the dynamometer in the background above and the coupling transmission in the photo below.

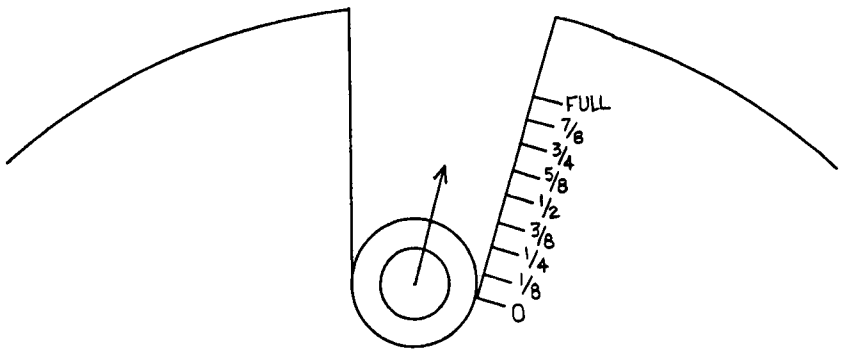


Figure 44. Rotation measurement increments.

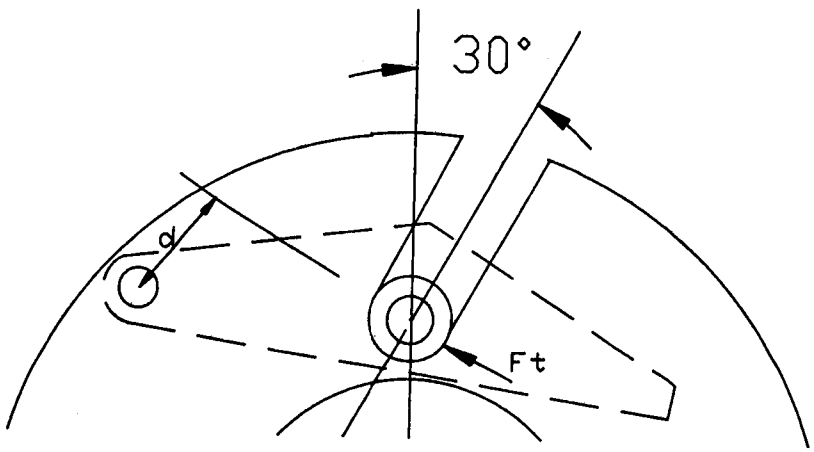


Figure 45. Illustration of the moment created by the torque reaction force for a large slot angle.

The 6 lb/in springs were originally installed on the mechanism. The static cam torque was determined by turning the cam shaft with a torque wrench (24 ft-lb). Because of this torque requirement and the light springs, the pivoting arms rotated with any rotation of the cam and would not return. The analysis confirmed this behavior of the mechanism. The analysis also showed that the 15 lb/in springs would not hold the arms at this torque either, but they were installed despite this fact. The arms did, indeed, move out when the cam rotation began. Instead of remaining there, they moved back down the slots approximately half way when the speed was increased. The only explanation for this behavior was a decrease in cam torque as speed increases. Calculations indicated that the running torque decreased to approximately one-third of its static value.

A second set of slots were cut in the plate at a 15° angle. This decreased the moment arm of the torque force. When the 6 lb/in springs were used on the mechanism, the arm would rotate immediately to the outer position at the speed required to overcome the preload. As the arm began its movement, the moment of the torque force increased faster than the moment applied by the springs. Therefore, the motion was unstable because the springs were insufficiently stiff. When the 9 lb/in springs were installed, the stiffness was sufficient to avoid the unstable motion and the

arms moved in the prescribed incremental motion. Several tests were run using both the 6 and 9 lb/in springs.

During the testing procedure, the behavior of the mechanism was found to be very sensitive to the angle and symmetry of the slots. Unsymmetrical slots caused binding because the arms did not rotate simultaneously. The cam torque would actually be transmitted by only one arm if the slots were not symmetric. As previously mentioned, the angle of the slot defines the moment produced by the torque reaction force. A small slot angle (<10° for the prototype) can produce a negative moment arm and, consequently, the arm will not rotate.

An independent dynamic analysis program was developed for the specific geometry of the prototype. All of the parameters were known at this point, except the actual cam torque and friction coefficient of the pivot pin. These two unknowns were varied until the output for the 9 lb/in spring fit the experimental data relatively well. Next, the program was run for the 6 lb/in spring to observe how well its output fit the corresponding data. The friction and cam torque were then altered slightly to improve its fit. The process continued until the set of parameters which best fit both sets of data were found (torque force--48 lb, coefficient of friction--.24). The torque force has a much greater bearing on the behavior of the mechanism than friction,

and this torque agrees with the reduced cam torque discovered earlier when heavy springs were employed. Figures 46 and 47 show the comparison of the experimental and analytical curves for the motion of the pivoting arms and resulting cam rotation. The curves were developed from the tabulated experimental data given in Table 4.

D. Sources of Error

Having determined approximations for the unknown cam torque and coefficient of friction, the remaining variations between the experimental and analytical results could be explained by several other sources of error.

1. Readability of instruments

a. Error in reading the percentage of arm rotation where the least count was 12.5%.

b. Error in reading the stroboscope with least count of 10 rpm.

2. Other factors

a. The additional friction surface between the back side of the pivoting arms and the cam gear.

b. The twisting of the arm resulting from non-coplanar forces. The analysis was totally two-dimensional.

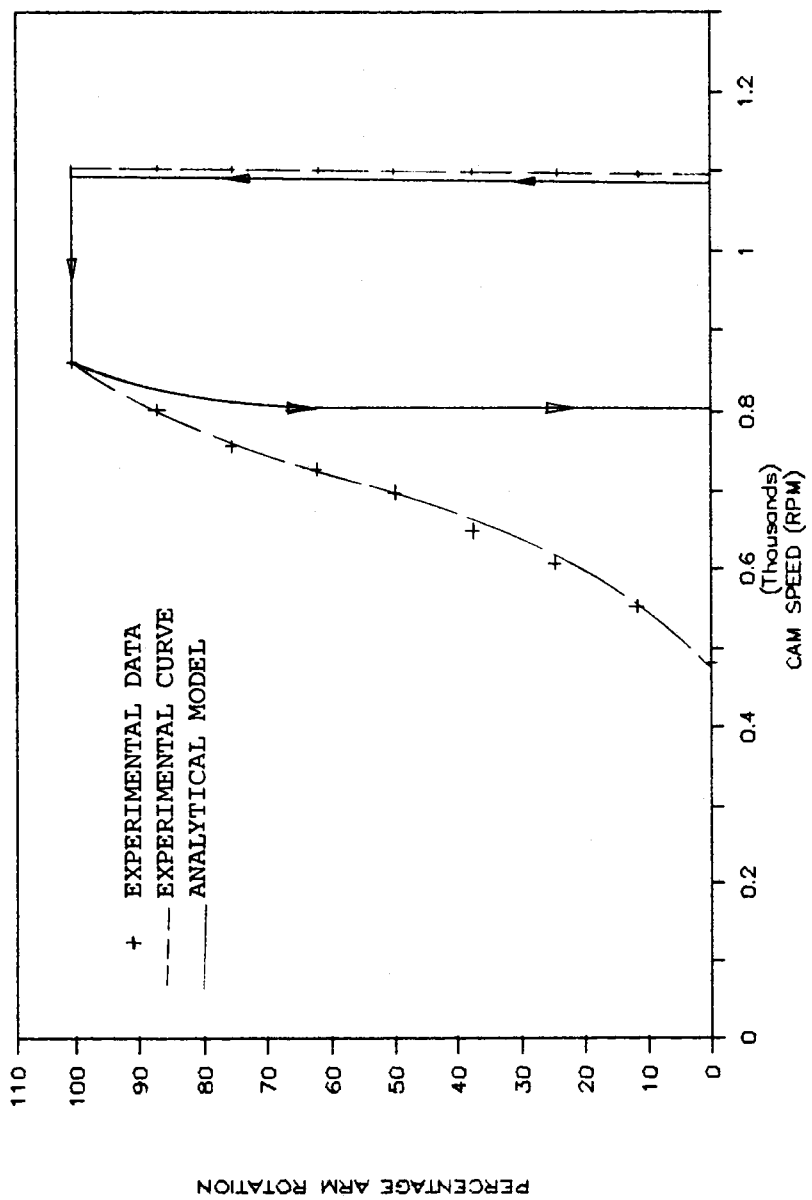


Figure 46. Experimental and theoretical curves for the motion utilizing the (6 lb/in, 5 lb preload) springs on the mechanism.

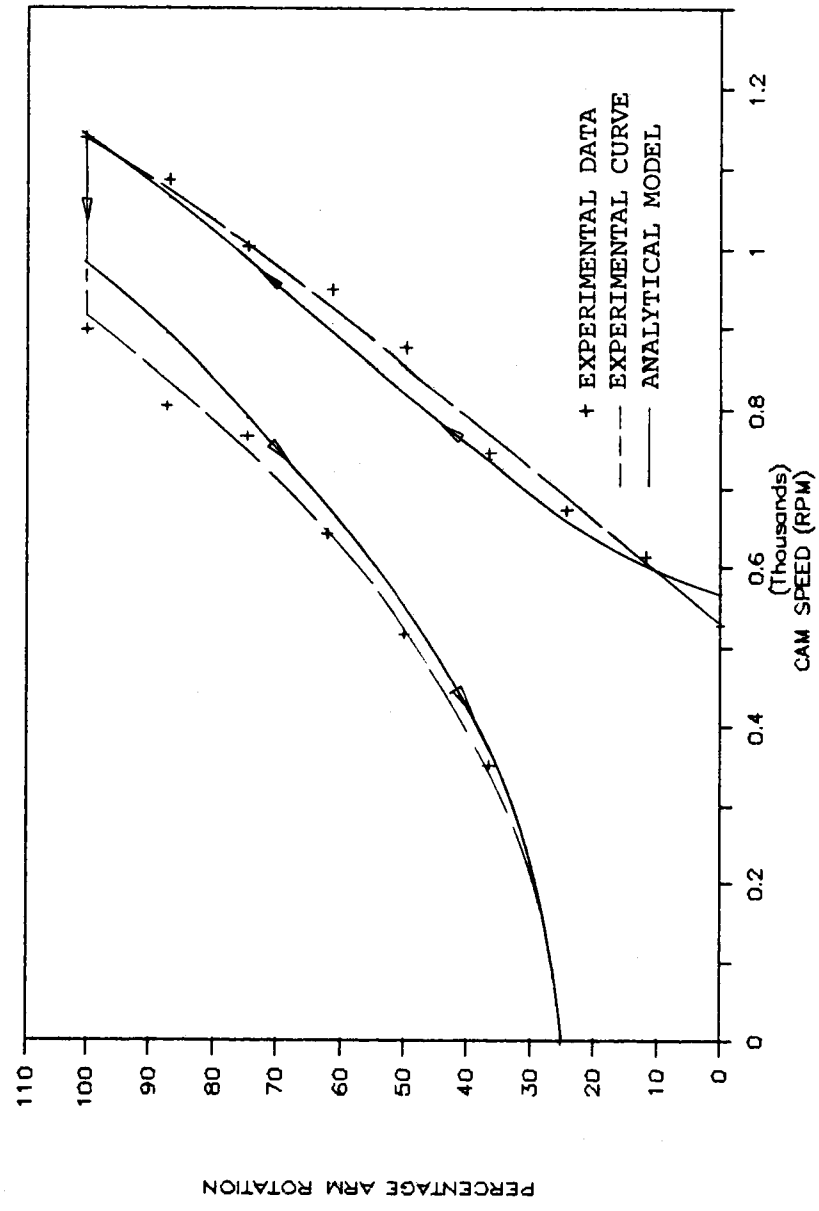


Figure 47. Experimental and theoretical curves for the motion utilizing the (9 lb/in, 3 lb preload) springs on the mechanism.

TABLE 4. EXPERIMENTAL DATA AND PROGRAM OUTPUT

%.RETARDED	CAM SPEED(RPM) TEST 1	TEST 2	TEST 3	PROGRAM OUTPUT	AVERAGE DATA
	PART 1 - 9 LB/IN SPRING				
0	500	530		563	
12	--	615		601	
25	650	670		668	
37	750	750		744	
50	900	880		821	
62	--	950		907	
75	1000	1000		983	
87	--	1080		1059	
100	1100	1130		1136	
100	900	900		983	
87	--	810		897	
75	750	770		792	
62	--	640		678	
50	500	510		544	
37	300	350		372	
25	0	0		0	
12	0	0		0	
0	0	0		0	
	PART 2 - 6 LB/IN SPRING				
0	1160	1220	1200	1184	1193
12	1160	1220	1200	1184	1193
25	1160	1220	1200	1184	1193
37	1160	1220	1200	1184	1193
50	1160	1220	1200	1184	1193
62	1160	1220	1200	1184	1193
75	1160	1220	1200	1184	1193
87	1160	1220	1200	1184	1193
100	1160	1220	1200	1184	1193
100	--	800	850	850	850
87	--	--	--	830	805*
75	--	--	760	811	760
62	--	--	--	802	725*
50	--	--	690	802	690
37	--	--	--	802	647*
25	--	--	605	802	605
12	--	--	--	802	542*
0	570	470	480	802	480

* INTERPOLATED VALUE

CHAPTER 6

FAILURE ANALYSIS

A. Analysis of Load Bearing Parts

A stress analysis of each loaded part in the mechanism was performed to check the factors of safety. The calculations, given in Appendix C, revealed large safety factors for each loaded part excluding the springs. The springs should be safe for a limited number of cycles (<1,000) before the bending stress begins to yield the end loops.

Part	Factor of Safety
Bearing Shaft	3.66
Pivot Pin	8.80
Bolts	8.00

B. Consequences of Failure

In the event of the failure of any part, the consequences should be known and understood. The following explanations outline the consequences of each conceived failure in the mechanism.

1. Breakage of one spring--If one spring is broken before the arm has rotated out, the arm will immediately

rotate until it hits the natural stop formed by the timing gear. The entire load will then be carried by the other arm and bearing. The increased torque reaction force on this arm will cause it to begin rotation at a lower speed. This increased force should not cause any further failures to occur on the load bearing parts of that arm.

2. Breakage of both springs--If both of the springs were to fail simultaneously at any speed, the arms would immediately move out, rotate the cam, and remain there until the device was disassembled. Because of the size of the specified springs and the limited space underneath the drive plate, there would no chance of the springs "flying out" of the cam gear and contacting the timing cover. There was a chance of this in the prototype design where the springs were not covered by the gear. The torque force on each bearing would remain unchanged.

3. One bearing shaft failure--The breakage or failure of the press fit would result in the bearing and shaft being moved out radially by the centrifugal force. The cam gear and timing cover should restrict any further movement of either. In the event that either the shaft or the bearing did get past the interior of the cam gear, it would fall into the oil pan. The torque would be transmitted by the opposite arm and bearing as in the case of one broken spring.

4. failure of both bearing shafts--In the unlikely event that both shafts are broken, the mechanism would have no source to transmit any torque to the cam shaft and engine failure would result.

CHAPTER 7

COST ANALYSIS

A cost analysis for the cam retarding mechanism was performed assuming the production of one hundred assemblies. The time required for set-up and machining of each part was estimated from the prototype fabrication. Current prices for round stock and flat steel were used to calculate the approximate cost of material needed for the assemblies. Refer to Tables 5 through 8 for the individual and total cost of fabrication. The approximate cost of each assembly was estimated at two hundred and eighty-five dollars.

TABLE 5. LABOR AND MACHINING COST

Labor and Machining Rate - $35.00/hr

PART	Ts	Tm	TOTAL
GEAR	2.5	75	77.5
ARMS	4.0	250	254
PINS	1.0	50	51
SHAFTS	1.0	50	51
SPACER	1.5	250	251.5
PLATE	3.0	100	103
TOTAL HOURS			788
TOTAL COST			$27580.00

Ts - MACHINE SET-UP TIME(HR)
Tm - MACHINING TIME * 100 PARTS

TABLE 6. MATERIAL COST

RAW MATERIAL COST

STEEL FOR GEAR - $29.00/FT
STEEL FOR PLATE - $29.00/FT
STEEL FOR SPACER - $4.30/FT
STEEL ROD FOR PINS AND SHAFTS - $0.75/FT
STEEL PLATE FOR ARMS - $7.70/SQ FT

PART	MR	MR100	COST
GEAR	.625IN	5.2FT	$150.80
ARMS	2.5SQ IN	1.62SQ FT	$12.47
PINS	.6625IN	5.5FT	$4.13
SHAFTS	.7625IN	6.35FT	$4.76
SPACER	1.5IN	12.5FT	$53.75
PLATE	.20IN	1.70FT	$49.30
TOTAL COST			$275.21

MR - MATERIAL REQUIRED PER PART
MR100 - MATERIAL REQUIRED FOR 100 PARTS

TABLE 7. PREFABRICATED PART COST

PART	QUANTITY	COST
SPRINGS	200	$50.00
BOLTS	300	$75.00
BEARINGS	200	$460.00
SNAP RINGS	200	$92.00
TOTAL COST		$677.00

TABLE 8. TOTAL COST

LABOR AND MACHINING COST	$27580.00
MATERIAL COST	$275.21
PREFABRICATED PART COST	$677.00
TOTAL COST FOR 100 ASSEMBLIES	$28532.21
COST PER ASSEMBLY	$285.21

CHAPTER 8

SUMMARY

A. Conclusions

The intent of this project was to design a cam timing delay mechanism which would operate predictably and meet as many of the desired specifications as possible. As seen in the comparison curves of the cam speed versus cam rotation, the analytical model was successful in predicting the motion of the prototype cam retarder once the approximate cam torque had been determined. One valuable discovery extending from the project was the significant decrease in the cam torque as the engine speed increased. The most disappointing conclusion made in the project was the fact that the designed mechanism would not fit in the provided space of a stock engine. The proposed design, although more compact than the prototype built, will not fit in the space between the stock cam gear and the timing cover. The torque dependency of the design was effectively minimized to the point where a change in the torque would not cause a major variation in rotation speeds. Despite extensive efforts to obtain the best effective spring, one could not be designed for infinite life in the mechanism. According to the

stress-life diagram for round steel wire, the springs specified would last, at maximum, 1000 cycles. The life of the springs could be extended by using a lighter weight and spring combination. Unfortunately, this would significantly increase the torque sensitivity of the mechanism.

B. Recommendations

Future studies in this area of totally mechanical cam timing delay could include the possible design of a cam retarder, timing cover, and pulley system. Such a system would not confine the designer to such stringent space limitations. The cam torque reduction with increased engine speed could be studied, possibly, to discover ways of decreasing the power used in driving the cam shaft. The information on cam torque in this report could also be helpful in other design areas. Utilizing the cam retarder design, important studies could be done on the actual increase in performance for different rotation angles and at variable operating speeds.

LIST OF REFERENCES

LIST OF REFERENCES

1. Automotive Engineering Magazine. "Camshaft Phase Adjuster Varies Valve Timing." July 1986, pp. 62-63.

2. Design Handbook--Springs, Custom Metal Parts. Associated Spring Corporation, Bristol, Connecticut, 1970.

3. Johnston, Russell E. and Ferdinand P. Beer. Mechanics of Materials. McGraw-Hill Book Company, 1981, pp. 574-578.

4. Juvinall, Robert C. Fundamentals of Machine Component Design. John Wiley and Sons, Inc., 1983, pp. 351-386.

5. Moisan, Richard. "Design of a Camshaft Gear for a Variable Valve Timing in a 350 Cubic Inch Displacement Chevrolet High Performance Engine." (Unpublished design project, The University of Tennessee, Knoxville, 1987.)

6. Spotts, M. F. Design of Machine Elements. Prentice-Hall, Inc., Englewood Cliffs, New Jersey, 1985.

7. Timoshenko, S. Strength of Materials--Part 1. D. Van Nostrano Company, Inc., Princeton, New Jersey, 1956, pp. 378-379.

8. Timoshenko, S. Strength of Materials--Part 2. D. Van Nostrano Company, Inc., Princeton, New Jersey, 1956, p. 28.

APPENDIXES

APPENDIX A

BEAM STRESS CALCULATIONS

CANTILEVER BEAM CALCULATIONS

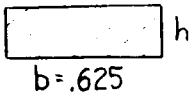


Figure A-1. Beam cross-section.

SPRING RATE--40 LB/IN
BEAM LENGTH--2.0 IN
BEAM DEFLECTION--0.5 IN

$$K = \frac{3EI}{L^3}$$

$$P = K\delta = 40(.5) = 20 \text{ LB}$$

$$I = \frac{bh^3}{12} = \frac{.625h^3}{12}$$

$$E = 30 \times 10^6 \text{ PSI}$$

$$K = 40 = \frac{3(30\times10^6)\ .625h^3}{(2.0)^3 \quad 12}$$

SOLVE FOR h

$$h = 0.04 \text{ IN}$$

$$I = \frac{.625(.04)^3}{12} = 3.33 \times 10^{-6} \text{ IN}^4$$

$$M = PL = 20(2) = 40 \text{ IN-LB}, \quad c = h/2 = .02 \text{ IN}$$

$$\sigma_b = \frac{Mc}{I} = \frac{40(.02)}{3.33\times10^{-6}} = 240{,}000 \text{ PSI}$$

K = spring rate
P = load
I = moment of inertia
E = elastic modulus
M = moment
σ_b = bending stress

STRAIGHT BEAM CALCULATIONS

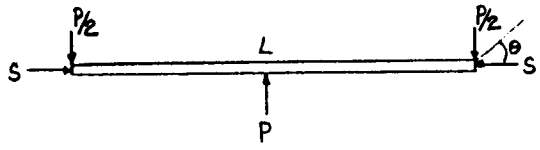


Figure A-2. Free-body diagram.

LOAD, P = 20LB

BEAM LENGTH, L = 3.5 IN

AXIAL COMPONENT OF REACTION, S = P/2COT(θ) = 9.05 LB

DEFLECTION,

$$Y_{max} = \frac{PL}{48EI} \times \frac{\tan u - u}{1/3\ u^3} \qquad \text{where } u^2 = \frac{SL^2}{4EI}$$

ESTIMATE

$$Y_{max} = \frac{PL^3}{48EI}$$

SOLVE FOR I = 4.47×10^{-6} IN^4

$$I = \frac{bh^3}{12} = \frac{.625h^3}{12} = 4.47 \times 10^{-6}\ IN^4$$

SOLVE FOR h = .004 IN

$$u^2 = 0.47$$

MOMENT, $M_{max} = \frac{PL}{4} \times \frac{\tan u}{u} = 18.91$ IN-LB

BENDING STRESS, $\sigma_b = \frac{Mc}{I} = 93{,}087$ PSI

CURVED BEAM CALCULATIONS

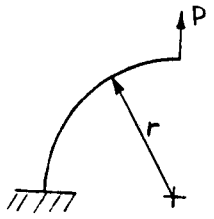


Figure A-3. Curved beam configuration.

DEFLECTION, $Y = \frac{\pi P r^3}{4EI}$

LOAD, P = 20 LB

RADIUS, r = 1.25 IN

DEFLECTION, y = 0.5 IN

SOLVE FOR I = 4.09×10^{-6} IN^4

$$I = \frac{bh^3}{12} = \frac{.625h^3}{12} = 4.09 \times 10^{-6} \text{ IN}^4$$

SOLVE FOR h = .0428 IN

$$c = \frac{2r}{h} = 58.4$$

$$k_c = \frac{3c^2-c-0.8}{3c(c-1)} = 1.011$$

$$\sigma_{max} = k_c \frac{6M}{bh^3} + P/A$$

MOMENT, M = Pr = 25 IN-LB, B = .625 IN

AREA, A = bh = .0267 IN^2

$$\sigma_{max} = 133,274 \text{ PSI}$$

APPENDIX B

THEORETICAL ANALYSIS

A. CENTRIFUGAL FORCE

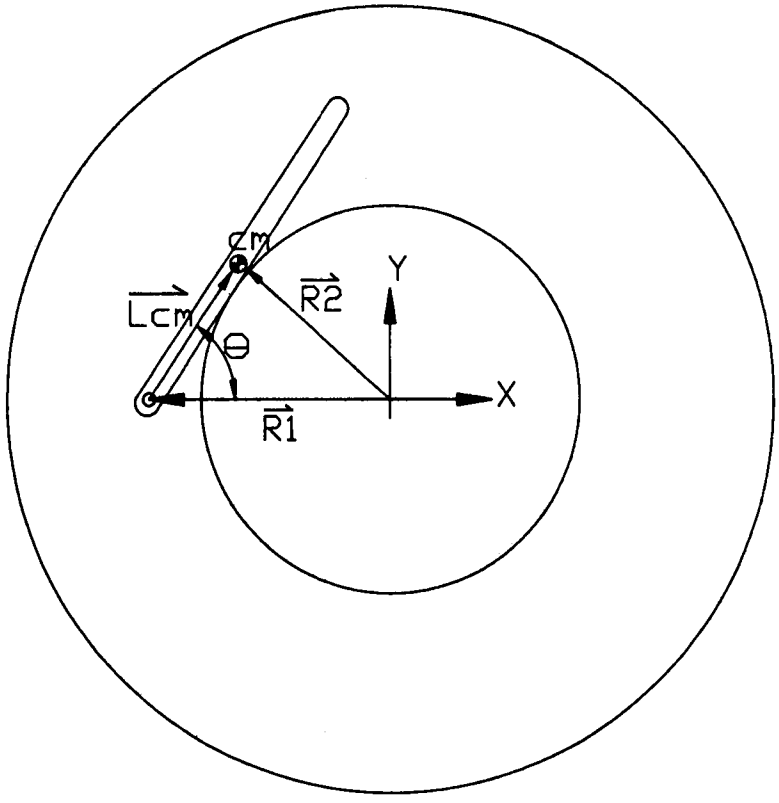


Figure B-1. Vectors defining the location of the center of mass.

$$R2^2 = R1^2 + L_{cm}^2 - 2(R1)(L_{cm})\cos\theta \qquad (A1)$$

$$F_{CENT} = mrw^2 = m(R2)w^2 \qquad (A2)$$

VECTORS

$\vec{R1} = (-R1, 0)$

$\vec{L}_{cm} = (L_{cm}\cos\theta,\ L_{cm}\sin\theta)$

$$\vec{R2} = \vec{R1} + \vec{L}_{cm} \qquad \text{(A3)}$$

$$= (-R1 + L_{cm} \cos\theta,\ L_{cm} \sin\theta)$$

$$\vec{F}_{CENT} = m(R2)w^2 \frac{\vec{R2}}{|R2|} = mw^2\vec{R2} \qquad \text{(A4)}$$

B. ARM ANGLES RELATIVE TO X-AXIS

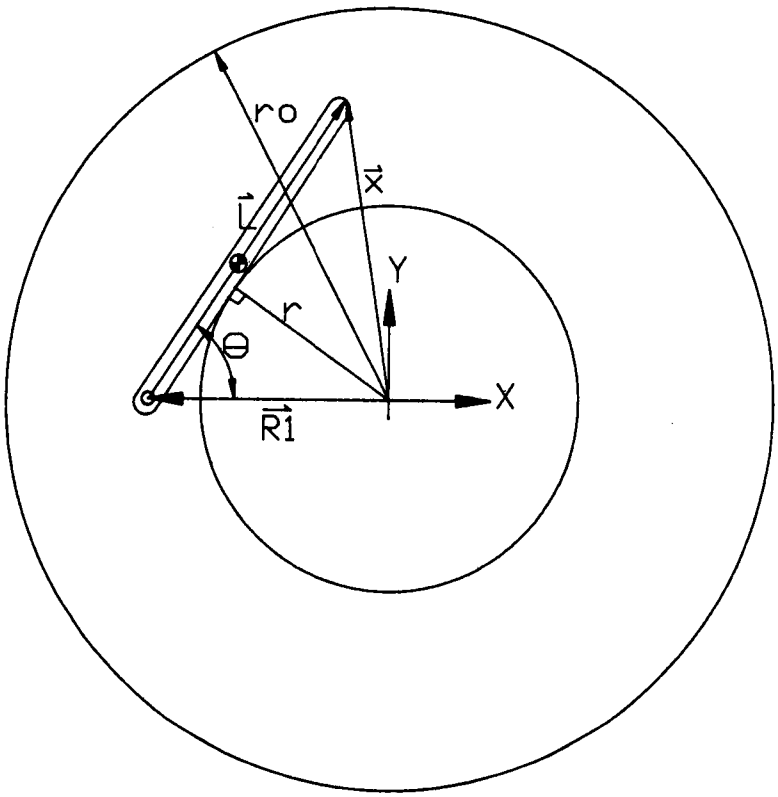


Figure B-2. Vectors defining minimum and maximum arm angle.

MINIMUM OR INITIAL VALUE OF θ

$$\frac{\sin 90}{R1} = \frac{\sin \theta}{r}$$

$$\theta_1 = \sin^{-1} \frac{r}{R1} \tag{A5}$$

MAXIMUM VALUE OF θ

$$\vec{x} = \vec{R1} + \vec{L}$$

$$|\vec{x}| \leq r_0$$

$$|\vec{R1} + \vec{L}| \leq r_0$$

$$\vec{L} = (L\cos\theta, L\sin\theta)$$

$$\vec{R1} + \vec{L} = (L\cos\theta - R1, L\sin\theta)$$

$$r_0^2 = (L\cos\theta - R1)^2 + (L\sin\theta)^2$$

$$r_0^2 = L^2\cos^2\theta - 2R1L\cos\theta + R1^2 + L^2\sin^2\theta$$

$$r_0^2 = L^2 + R1^2 - 2R1L\cos\theta$$

$$\theta_{max} = \cos^{-1} \frac{L^2 + R1^2 - r_0^2}{2R1L} \tag{A6}$$

C. SPRING FORCE

Assuming the spring force is approximately perpendicular to the arm in its initial position.

$$\vec{F}_{sp} = (F_{sp}\sin\theta, -F_{sp}\cos\theta)$$

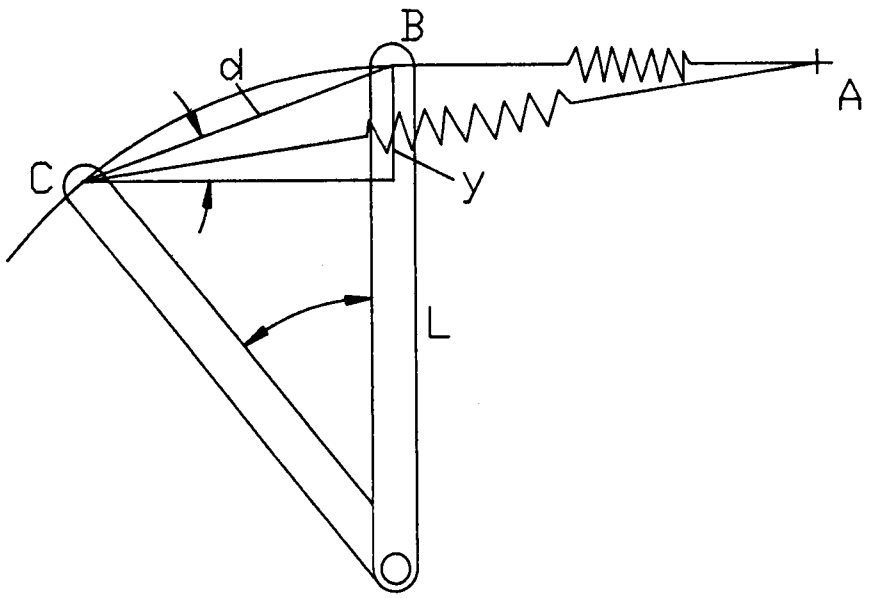


Figure B-3. Spring deflection.

D. TOTAL DEFLECTION OF THE SPRING

$$\alpha = \theta_{max} - \theta_{max}$$

$$d^2 = L^2 + L^2 = 2LL\cos\alpha$$

$$d = \sqrt{2L^2-2L^2\cos\alpha}$$

$$y = L-L\cos\alpha$$

$$d\sin\phi = L - L\cos\alpha$$

$$\phi = \sin^{-1} \frac{L-L\cos\alpha}{d}$$

AB--INITIAL LENGTH OF SPRING

$$\vec{AB} + \vec{BC} = \vec{AC}$$

$$\vec{AC} = (AB + d\cos\phi,\ d\sin\phi)$$

$$|\vec{AC}| = \sqrt{(AB+d\cos\phi)^2 + (d\sin\phi)^2} \qquad \text{(A7)}$$

SPRING DEFLECTION

$$\delta = AC - AB \qquad \text{(A8)}$$

E. CAM TORQUE REACTION FORCE

$$\vec{L}_p = (L_p\cos\theta,\ L_p\sin\theta)$$

$$\vec{R3} = \vec{R1} + \vec{L}r$$

$$\vec{R3} = (L_p\cos\theta - R1,\ L_p\sin\theta)$$

$$R3 = \sqrt{(L_p\cos\theta - R1)^2 + (L_p\sin\theta)^2} \qquad \text{(A9)}$$

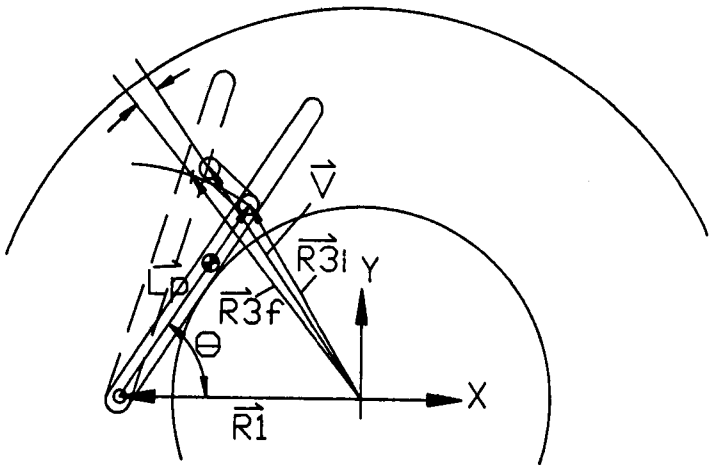


Figure B-4. Vectors defining pin position.

$\vec{R3}_i$ = initial vector for $\theta = \theta_{min}$

$\vec{R3}_f$ = final vector for $\theta = \theta_{max}$

β = cam rotation angle

$$|\vec{v}| = |\vec{R3}_f|$$

$$AR3 = \text{Angle of } \vec{R3}_f = \tan^{-1} \frac{R3y}{R3x}$$

$$= \tan^{-1} \frac{L_p \sin\theta}{L_p \cos\theta - R1} \qquad \text{(A10)}$$

$$AV = \text{angle of } \vec{v} = AR3 - \beta \qquad \text{(A11)}$$

$$\vec{v} = (R3_f \cos(AV),\ R3_f \sin(AV))$$

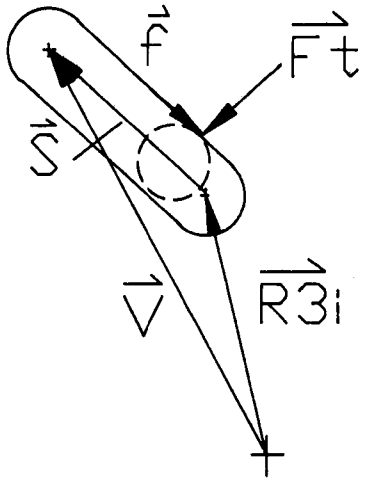


Figure B-5. Vectors defining friction force and torque reaction force direction.

SLOT VECTOR $\vec{S} = \vec{V} - \vec{R3}_i$

$$\vec{S} = (V_x - R3_{ix},\ V_y - R3_{iy}) = (S_x, S_y) \qquad \text{(A12)}$$

SLOT VECTOR ANGLE = SA = $\tan^{-1} \frac{Sy}{Sx}$

$$|\vec{S}| = \sqrt{Sx^2 + Sy^2} \qquad \text{(A13)}$$

THE ANGLE OF THE TORQUE REACTION FORCE

$$TA = SA + 90° \qquad \text{(A14)}$$

TORQUE VECTOR

$$\vec{F}_t = \frac{T}{R3} (\cos TA,\ \sin TA)$$

magnitude only is a function of θ.

F. FRICTION FORCE

$$f = \mu F_T$$

$$f = \mu\left(\frac{T}{R3}\right) \tag{A15}$$

DIRECTION IS OPPOSITE OF SLOT VECTOR $\vec{S}$

$$\vec{f} = \mu\left(\frac{T}{R3}\right)\vec{w} \quad \text{where}$$

$$\vec{w} = \begin{cases} -\dfrac{\vec{S}}{|\vec{S}|} & \text{for increasing } \theta \\ +\dfrac{\vec{S}}{|\vec{S}|} & \text{for decreasing } \theta \end{cases} \tag{A16}$$

G. SPRING FORCE

LS = INITIAL LENGTH
OF SPRING

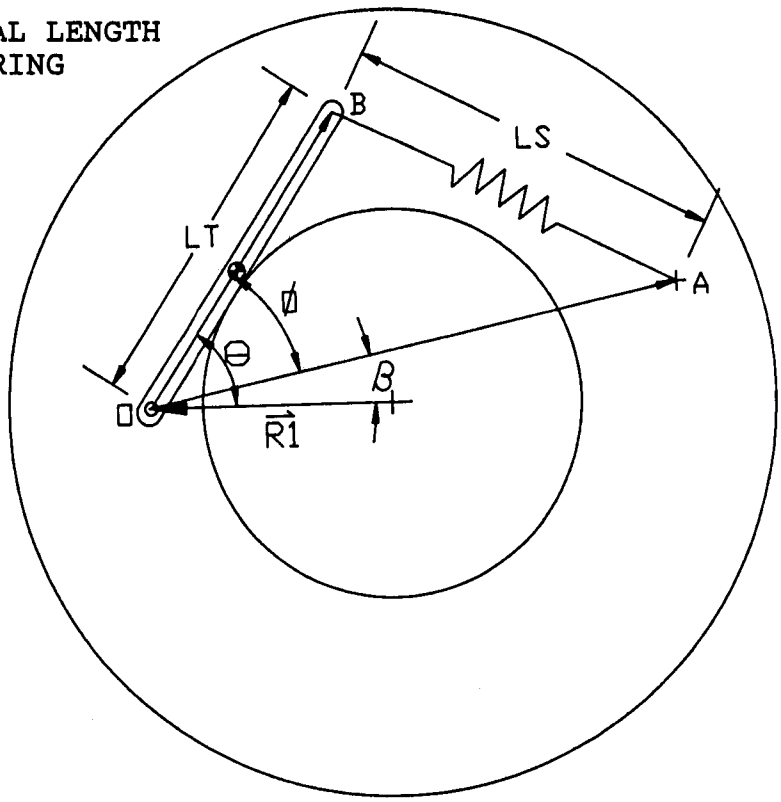


Figure B-6. Vectors defining spring force direction.

$$OA \simeq \sqrt{LT^2+LS^2}$$

$$\frac{\sin 90}{OA} = \frac{\sin \phi}{LS}$$

$$\phi = \sin^{-1} \frac{LS}{OA}$$

$$\beta_0 = \theta - \phi$$

$$\vec{O}A = (OA\cos\beta_0,\ OA\sin\beta_0)$$

$$\vec{OA} + \vec{AB} = \vec{OB}$$

$$\vec{AB} = \vec{OB} - \vec{OA}$$

$$\vec{OB} = (LT\cos\theta,\ LT\sin\theta)$$

$$\vec{AB} = (LT\cos\theta - OA\cos\beta_0,\ LT\sin\theta - OA\sin\beta_0) = (AB_x,\ AB_y)$$

$$AB = |\vec{AB}| = \sqrt{AB_x^2 + AB_y^2}$$

DEFLECTION OF SPRING, δ = AB-LS

f_0 = INITIAL PRELOAD OF THE SPRING

SPRING FORCE $F_{sp} = K\delta + f_0 = K(AB-LS) + f_0$

DIRECTION IS OPPOSITE TO AB

$$\vec{F}_{sp} = [f_0 + K(AB-LS)]\ (-\frac{\vec{AB}}{AB}) \qquad (A17)$$

H. INITIAL PRELOAD

Sum moments about pivot point 0 to calculate initial spring force rquired.

$$+ \Sigma M_0 = -F_{cx}L_{cm}\sin\theta + F_{cy}L_{cm}\cos\theta - (f_x+F_{tx})L_p\sin\theta$$
$$+ (f_y+f_{ty})Lp\cos\theta + F_{spx}LT\sin\theta + F_{spy}LT\cos\theta = 0$$

$$F_{spx} = f_{sp}\sin\theta$$

$$F_{spx} = f_{sp}\cos\theta$$

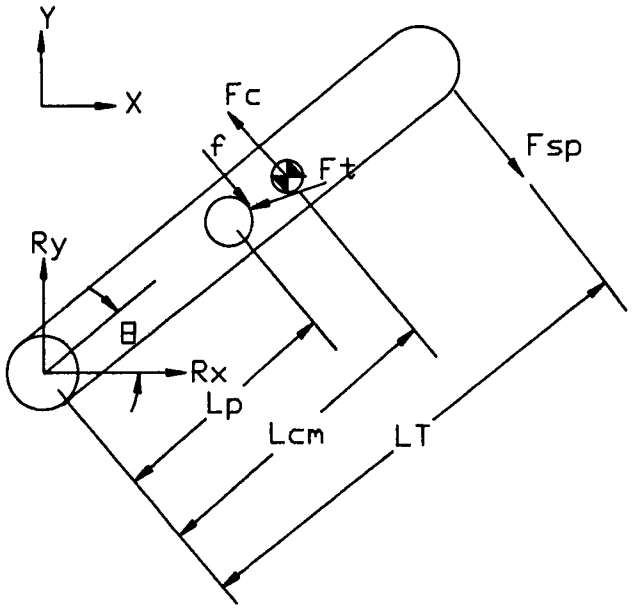


Figure B-7. Arm free body diagram.

$$+ \Sigma M_0 = F_{cx}L_{cm}\sin\theta + F_{cy}L_{cm}\cos\theta - (f_x+F_{tx})L_p\sin\theta + (f_y+F_{ty})L_p\cos\theta + F_{sp}L_T\sin^2\theta + F_{sp}L_T\cos^2\theta = 0$$

$$+ \Sigma M_0 = F_{cx}L_{cm}\sin\theta + F_{cy}L_{cm}\cos\theta - (f_x+F_{tx})L_p\sin\theta + (f_y+F_{ty})L_p\cos\theta + F_{sp}L_T = 0$$

INITIAL PRELOAD

$$f_o = F_{sp} = -\left[\frac{(-F_{cx}L_{cm} - (f_x+F_{tx})L_p)\sin\theta + (F_{cy}L_{cm} + (f_y+F_{ty})L_p)\cos\theta}{L_T}\right] \quad \text{(A18)}$$

I. SPRING CONSTANT

To solve for the spring constant and final spring force substitute equation (A17) for FSP into moment equation A solve for K with the total deflection being known from equation (A8).

$$\text{SPRING CONSTANT } K = F_{cx}L_{cm}\sin\theta - F_{cy}L_{cm}\cos\theta + (Fx + F_{tx})$$

$$\theta = \theta_{max}$$

$$+ \Sigma M_0 = -F_{cx}L_{cm}\sin\theta + F_{cy}L_{cm}\cos\theta - (fx+F_{tx})Lp\sin\theta$$

$$+ (fy+F_{ty})Lp\cos\theta - (f_0+k\delta)\left(-\frac{ABx}{AB}\right)LT\sin\theta$$

$$+ (f_0+k\delta)\left(-\frac{ABy}{AB}\right)LT\cos\theta = 0$$

$$\text{LET, } -F_{cx}L_{cm}\sin\theta + F_{cy}L_{cm}\cos\theta - (fx+F_{tx})Lp\sin\theta$$

$$+ (fy+F_{ty})Lp\cos\theta = M1$$

SOLVING FOR K YIELDS:

$$K = \frac{M1 + f_0\left(-\frac{ABx}{AB}\right)LT\sin\theta - f_0\left(-\frac{ABy}{AB}\right)LT\cos\theta}{\delta\left(-\frac{ABy}{AB}\right)LT\cos\theta - \delta\left(-\frac{ABx}{AB}\right)LT\sin\theta} \qquad \text{(A19)}$$

$$F_{sp}(\text{FINAL}) = f_0 + k\delta \qquad \text{(A20)}$$

APPENDIX C

PART FAILURE ANALYSIS

Stress Analysis of Load Bearing Parts

1. BEARING SHAFT

CAM TORQUE = 30 FT-LB
FORCE TRANSMITTED BY EACH BEARING, Fb=(15 FT-LB)/(.104 FT)=144 LB
ASSUMING BEARING DISTRIBUTES THE LOAD ALONG THE SHAFT;

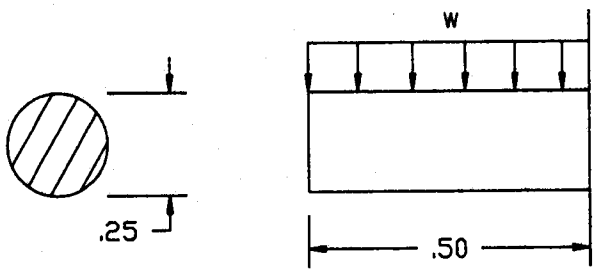


Figure C-1. Bearing shaft loading.

DISTRIBUTED LOAD, w=144LB/.5IN=288LB/IN
DISTANCE FFROM NEUTRAL AXIS,c=D/2=.125IN
MAXIMUM MOMENT, M=wL^2/2=36IN-LB
MOMENT OF INERTIA, I= R^4/2=3.83*10^-4
(BENDING STRESS),σ_b=Mc/I=11,735 PSI

AREA, A= R^2=.449IN^2
(TRANSVERSE SHEAR),τ=4P/3A=3910 PSI

Transverse shear is maximum at neutral axis. Therefore, the bending stress at the outer surface is the highest stressed area.

F.S. = Yield Strength/Maximum Stress
YIELD STRENGTH(1020 HOT-ROLLED STEEL)--43,000 PSI
FACTOR OF SAFETY--3.66

2. PIVOT PIN

THE MAXIMUM FORCE ON THE PIVOT PIN BY THE ROTATING ARM IS APPROXIMATELY 100 LB.

MOMENT, M=100*.15=15 IN-LB
c=D/2=.125
I=π/2*.125^4= 3.83*10^-4
σ_b= Mc/I = 4890 PSI

Factor of Safety = 8.8
Same situation for the transverse shear stress as before.

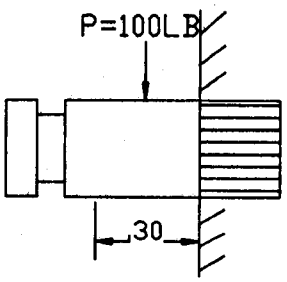


Figure C-2. Pivot pin loading.

3. BOLTS

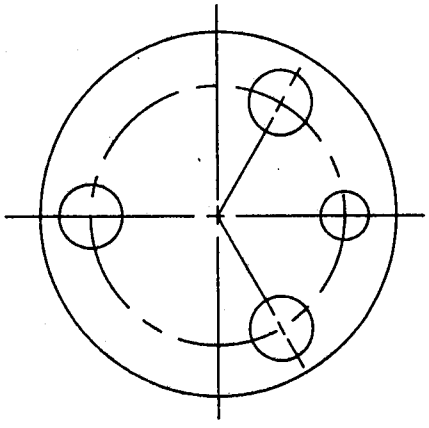


Figure C-3. Cam shaft bolt pattern and spacing.

TORQUE--30 FT-LB
TORQUE/BOLT--10 FT-LB
RADIUS FROM CENTER--.6875 IN
SHEARING FORCE/BOLT--175 LB
BOLT SPECIFIED--5/16"-18TPI
STRESS AREA--.0524 IN^2

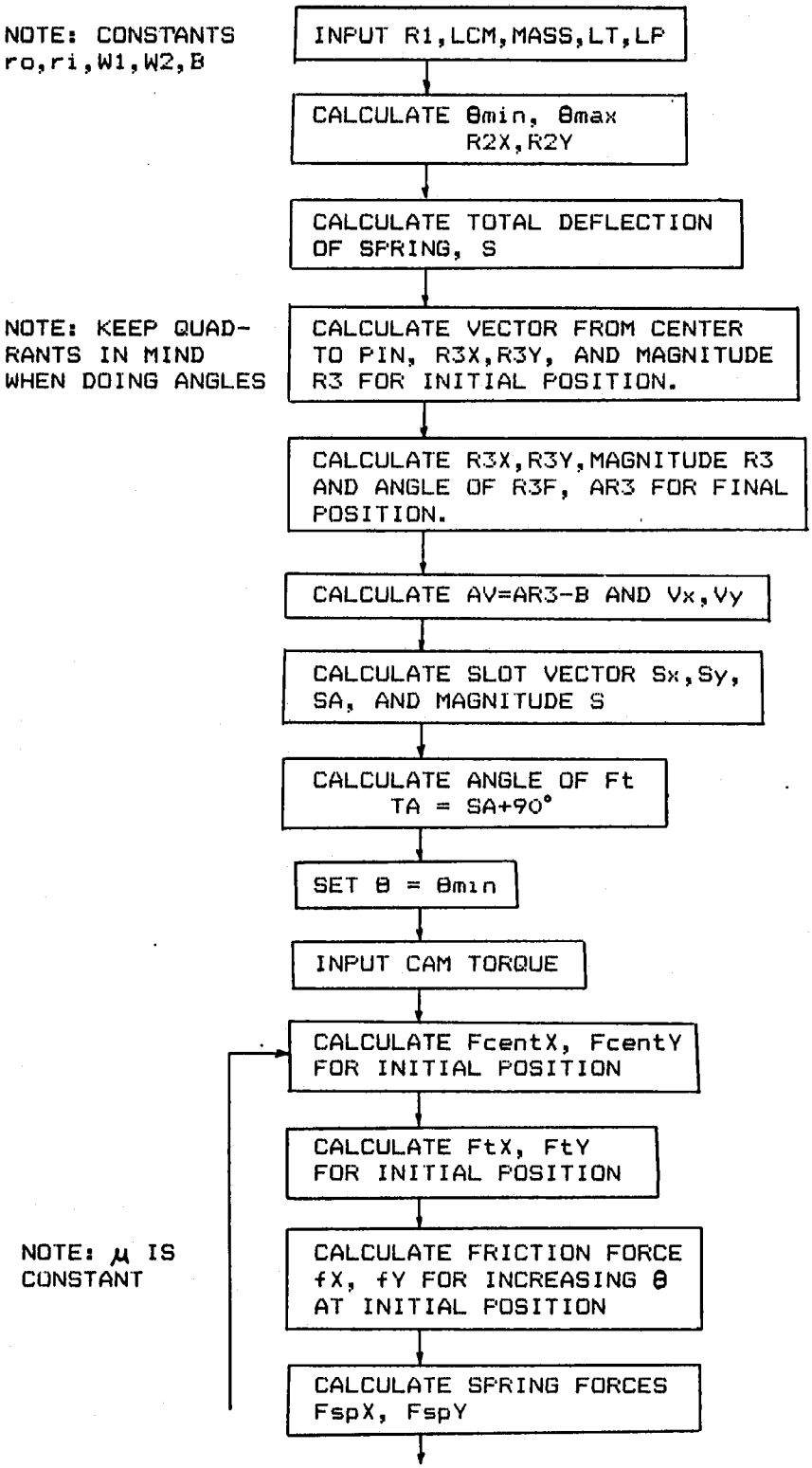
GRADE 1 BOLT YIELD STRENGTH--36,000 PSI
FACTOR OF SAFETY = 8

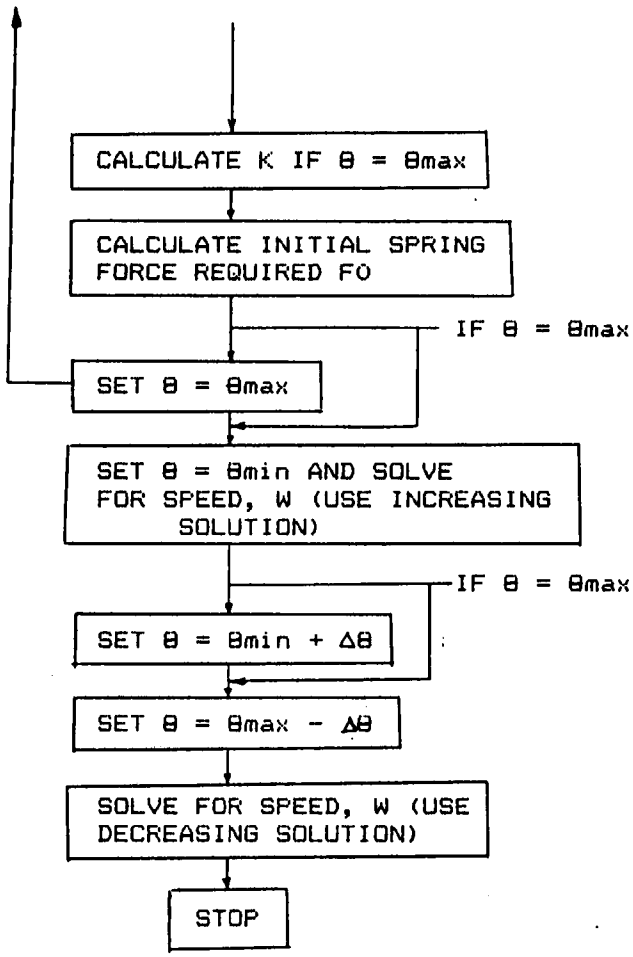
4. SPRINGS--SPRING STRESS AND FAILURE WAS ANALYZED IN CHAPTER 2.

APPENDIX D

COMPUTER PROGRAMS

Flow Chart


NOTE: CONSTANTS ro,ri,W1,W2,B
INPUT R1,LCM,MASS,LT,LP
CALCULATE θmin, θmax R2X,R2Y
CALCULATE TOTAL DEFLECTION OF SPRING, S
NOTE: KEEP QUADRANTS IN MIND WHEN DOING ANGLES
CALCULATE VECTOR FROM CENTER TO PIN, R3X,R3Y, AND MAGNITUDE R3 FOR INITIAL POSITION.
CALCULATE R3X,R3Y,MAGNITUDE R3 AND ANGLE OF R3F, AR3 FOR FINAL POSITION.
CALCULATE AV=AR3-B AND Vx,Vy
CALCULATE SLOT VECTOR Sx,Sy, SA, AND MAGNITUDE S
CALCULATE ANGLE OF Ft TA = SA+90°
SET θ = θmin
INPUT CAM TORQUE
CALCULATE FcentX, FcentY FOR INITIAL POSITION
CALCULATE FtX, FtY FOR INITIAL POSITION
NOTE: μ IS CONSTANT
CALCULATE FRICTION FORCE fX, fY FOR INCREASING θ AT INITIAL POSITION
CALCULATE SPRING FORCES FspX, FspY


CALCULATE K IF θ = θmax
CALCULATE INITIAL SPRING FORCE REQUIRED FO
IF θ = θmax
SET θ = θmax
SET θ = θmin AND SOLVE FOR SPEED, W (USE INCREASING SOLUTION)
IF θ = θmax
SET θ = θmin + Δθ
SET θ = θmax - Δθ
SOLVE FOR SPEED, W (USE DECREASING SOLUTION)
STOP

DYNAMIC ANALYSIS PROGRAM FOR CAM RETARDER

```
2 SCREEN 0,0,0
10 REM ************************************************************************
20 REM              CAM RETARDER LINK ANALYSIS PROGRAM
30 REM
40 REM   DAVID L. CONNER                                        DECEMBER 1987
50 REM ************************************************************************
55 REM PROMPT USER FOR INPUT
56 GOTO 71
60 PRINT "INPUT VARIABLES- MASS,RADIUS TO PIVOT,DISTANCE TO MASS CENTER,
         DISTANCE TO PIN, AND DISTANCE TO SPRING"
70 INPUT MASS,R1,LCM,LP,LT
71 MASS=.28:R1=2!:LCM=1.75:LP=.75:LT=3!
74 DIM W(50)
75 REM SPECIFY INNER AND OUTER RADIUS OF GEAR SPACE
80 RI=1!
90 RO=2.2
91 REM INPUT CAM TORQUE
92 PRINT "INPUT CAM TORQUE IN FT-LB"
93 INPUT T
94 T=T*12
95 REM DEVIDE TORQUE BY THE NUMBER OF PINS (2)
96 T=T/2
97 REM PROMPT USER ABOUT FRICTION CONSIDERATION
98 PRINT "DO YOU WANT TO INCLUDE FRICTION? YES-0,NO-1"
99 INPUT QQQ
100 REM SPECIFY OPERATING SPEEDS AND ROTATION ANGLE
101 W1=7100/2
110 W2=7700/2
111 REM CONVERT SPEEDS TO RADIANS PER SECOND
115 W1=W1*6.283185/60
116 W2=W2*6.283185/60
120 BETA=2*(3.14159/180)
125 REM CALCULATE MIN AND MAX PIVOT ANGLE
130 X=RI/R1
140 OMIN=ATN(X/SQR(-X*X+1))
150 X=(LT^2+R1^2-RO^2)/(2*R1*LT)
160 OMAX=-(ATN(X/SQR(-X*X+1)))+(3.14159/2)
165 REM CALCULATE MAXIMUM SPRING DEFLECTION
168 AB=2.14
170 X=OMAX-OMIN
180 D=SQR(2*LT^2-2*LT^2*COS(X))
190 Y=(LT-LT*COS(X))/D
200 Z=ATN(Y/SQR(-Y*Y+1))
210 AC=SQR((AB+D*COS(Z))^2+(D*SIN(Z))^2)
220 DELTA=AC-AB
221 LPRINT "DELTA=";DELTA
222 DELTA=.6
225 REM CALCULATE THE ANGLE OF THE SLOT
230 R3IX=-R1+LP*COS(OMIN)
240 R3IY=LP*SIN(OMIN)
250 R3I=SQR(R3IX^2+R3IY^2)
260 R3FX=-R1+LP*COS(OMAX)
```

```
270 R3FY=LP*SIN(OMAX)
280 R3F=SQR(R3FX^2+R3FY^2)
290 AR3=ATN(R3FY/R3FX)+3.14159
300 AV=AR3-BETA
310 VX=R3F*COS(AV)
320 VY=R3F*SIN(AV)
330 SX=VX-R3IX
340 SY=VY-R3IY
350 SA=ATN(SY/SX)+3.14159
360 S=SQR(SX^2+SY^2)
370 TA=SA+3.14159/2
405 REM SET THETA = MINIMUM VALUE TO CALCULATE INITIAL SPRING FORCE
410 O=OMIN
415 REM CALCULATE INITIAL TORQUE REACTION FORCES
420 FTX=T/R3I*COS(TA)
430 FTY=T/R3I*SIN(TA)
431 FT=SQR(FTX^2+FTY^2)
435 PRINT "TORQUE FORCES";FTX,FTY
440 REM CALCULATE INITIAL CENTRIFUGAL FORCES
450 R2X=-R1+LCM*COS(O)
460 R2Y=LCM*SIN(O)
470 FCX=MASS/386*R2X*W1^2
480 FCY=MASS/386*R2Y*W1^2
485 PRINT "CENT FORCES";FCX,FCY
520 IF QQQ=1 THEN 600
525 MU=.05
530 FRIC=MU*FT
540 FRICX=FRIC*(-SX/S)
550 FRICY=FRIC*(-SY/S)
560 PRINT "FRICT FORCES";FRICX,FRICY
600 REM CALCULATE INITIAL SPRING FORCE REQUIRED BY SUMMING MOMENTS
610 FSP=((-FCX*LCM-(FRICX+FTX)*LP)*SIN(O)+(FCY*LCM+(FRICY+FTY)*LP)*COS(O))/LT
625 FO=FSP
630 LPRINT "INITIAL SPRING FORCE RREQUIRED-";FSP
640 REM SET THETA = MAX VALUE AND SOLVE FOR SPRING CONSTANT
650 O=OMAX
659 REM CALCULATE FINAL TORQUE REACTION FORCES
660 FTX=T/R3F*COS(TA)
670 FTY=T/R3F*SIN(TA)
680 FT=SQR(FTX^2+FTY^2)
690 PRINT "TORQUE FORCES";FTX,FTY
691 REM CALCULATE FINAL CENTRIFUGAL FORCES
700 R2X=-R1+LCM*COS(O)
710 R2Y=LCM*SIN(O)
711 PRINT "R2=";SQR(R2X^2+R2Y^2)
720 FCX=MASS/386*W2^2*R2X
730 FCY=MASS/386*W2^2*R2Y
740 PRINT "CENT FORCES";FCX,FCY
750 REM CALCULATE FRICTION FORCES IF REQUIRED
760 FRIC=MU*FT
770 FRICX=FRIC*(-SX/S)
780 FRICY=FRIC*(-SY/S)
```

```
790 PRINT "FRICT FORCES";FRICX,FRICY
800 OA=SQR(LT^2+AB^2)
810 X=AB/OA
820 PHI=ATN(X/SQR(-X*X+1))
830 B1=OMIN-PHI
840 PX=LT*COS(O)-OA*COS(B1)
850 PY=LT*SIN(O)-OA*SIN(B1)
860 P=SQR(PX^2+PY^2)
870 FORCE=FCX*LCM*SIN(O)-FCY*LCM*COS(O)+(FRICX+FTX)*LP*SIN(O)-(FRICY+FTY)*LP*COS(O
880 AA=FORCE+FSP*(-PX/P)*LT*SIN(O)-FSP*(-PY/P)*LT*COS(O)
890 BB=DELTA*(-PY/P)*LT*COS(O)-DELTA*(-PX/P)*LT*SIN(O)
900 K=AA/BB
901 PRINT "K =";K
905 REM CALCULATE SPRING FORCES USING THE SPRING CONSTANT AND DEFLECTION
910 FSPX=(FSP+K*DELTA)*(-PX/P)
920 FSPY=(FSP+K*DELTA)*(-PY/P)
930 PRINT "SPRING FORCES";FSPX,FSPY
935 LPRINT "ANGLE   SPEED(RPM)"
940 REM STEP THE ROTATION ANGLE AND CALCULATE THE CORRESPONDING SPEED
950 O=OMIN
955 I=1
960 DO=(OMAX-OMIN)/10
970 PX=LT*COS(O)-OA*COS(B1)
980 PY=LT*SIN(O)-OA*SIN(B1)
990 P=SQR(PX^2+PY^2)
1000 DELTA=P-AB
1010 FSP=K*DELTA+FO
1020 FSPX=FSP*(-PX/P)
1030 FSPY=FSP*(-PY/P)
1040 R3X=-R1+LP*COS(O)
1050 R3Y=LP*SIN(O)
1060 R3=SQR(R3X^2+R3Y^2)
1070 FTX=(T/R3)*COS(TA)
1080 FTY=(T/R3)*SIN(TA)
1090 R2X=-R1+LCM*COS(O)
1100 R2Y=LCM*SIN(O)
1110 IF QQQ=1 THEN 1200
1120 IF I>11 THEN 1170
1130 FRICX=MU*(T/R3)*(-SX/S)
1140 FRICY=MU*(T/R3)*(-SY/S)
1160 GOTO 1200
1170 FRICX=MU*(T/R3)*(SX/S)
1180 FRICY=MU*(T/R3)*(SY/S)
1200 J1=(FRICX+FTX)*LP*SIN(O)-(FRICY+FTY)*LP*COS(O)+FSPX*LT*SIN(O)-FSPY*LT*COS(O)
1205 IF J1<0 THEN 1300
1210 J2=(MASS/386)*R1*LCM*SIN(O)
1220 OMEGA=SQR(J1/J2)
1230 W(I)=OMEGA*60/6.28318
1240 LPRINT O,W(I)
1250 I=I+1
1260 IF I>11 THEN 1300
1270 O=O+DO
```

```
1280 GOTO 970
1300 IF I>21 THEN 1400
1305 IF O<OMIN THEN 1400
1310 O=O-DO
1320 GOTO 970
1400 HY=W(1)-W(21)
1410 PRINT "R1=";R1
1420 PRINT "HYSTERESIS DIFFERENCE -";HY
1470 END
```

PROTOTYPE ANALYSIS PROGRAM

```
10 REM ******************************************************
20 REM  PROTOTYPE PREDICTION PROGRAM
30 REM ******************************************************
40 K=10
50 WT=.1
60 L1=1.88
70 L2=1.25
80 LC=1.23
90 LSP=2.43
100 OMIN=.733
110 OMAX=1.038
120 O=OMIN
125 W=0
130 VX=L2*COS(O)-L1
140 VY=L2*SIN(O)
150 M=WT/386
160 L2X=L2*COS(O)
170 L2Y=L2*SIN(O)
180 FCX=M*W^2*VX
190 FCY=M*W^2*VY
200 MC=L2X*FCY-FCX*L2Y
210 T=144/(SQR(VX^2+VY^2))
220 TX=-T*SIN(.9075)
230 TY=-T*COS(.9075)
240 DX=1.5*COS(O)
250 DY=1.5*SIN(O)
300 MT=TY*DX-TX*DY
310 ALPHA=O-.1248
320 SX=-2*L1+LSP*COS(ALPHA)
330 SY=LSP*SIN(ALPHA)
340 S=SQR(SX^2+SY^2)
350 IF O>OMIN THEN 400
360 S0=S
370 F0=9
400 FSPX=(F0+K*(S-S0))*-(SX/S)
410 FSPY=(F0+K*(S-S0))*-(SY/S)
500 MSP=LSP*COS(ALPHA)*FSPY-LSP*SIN(ALPHA)*FSPX
510 SUM=MC+MT+MSP
520 IF SUM>0 THEN 550
530 W=W+1
540 GOTO 180
550 PRINT W*9.5493 ,MC,MT,MSP,SUM,O
560 O=O+.01
570 GOTO 125
```

COMPRESSION SPRING ANALYSIS PROGRAM

```
10 REM ******************************************************
20 REM *            SPRING DESIGN PROGRAM FOR CAM RETARDER
30 REM ******************************************************
40 REM SET CONSTANTS FOUND FROM ANALYSIS PROGRAM
50 K=40
60 F0=28.2
70 DMAX=5/8
80 DELTA=.6
90 FMAX=F0+K*DELTA
100 CLASH=.1*FMAX/K
110 DW=.05
120 C=(DMAX-DW)/DW
130 KS=1+.615/C
140 TMAX=(8*FMAX*(DMAX-DW)*KS)/(3.14159*DW^3)
141 TMIN=(8*F0*(DMAX-DW)*KS)/(3.14159*DW^3)
145 G=11500000#
150 N=(DW^4*G)/(K*(DMAX-DW)^3*8)
160 N=N+2
170 SOLID=DW*N
180 PRINT DW,TMAX,TMIN,SOLID
190 DW=DW+.01
200 IF DW>.25 THEN 220
210 GOTO 120
220 END
```

DRAWBAR SPRING ANALYSIS PROGRAM

```
10 REM ***************************************
20 REM      MAXIMUM SPRING DESIGN PROGRAM
30 REM ***************************************
35 DEL=.4
40 F0=10
50 D=.01
60 N=5
65 G=11500000#
70 X=((.1*F0*8*(.425-D)^3*N)/(D^4*G))+(N*D)
80 IF ABS(X-1.56)<.01 THEN 200
90 D=D+.005
100 IF D>.15 THEN 120
110 GOTO 70
120 N=N+.25
125 D=.01
126 IF N>20 THEN 150
130 GOTO 70
150 F0=F0+2
160 N=5
170 D=.01
180 IF F0>75 THEN 250
190 GOTO 70
200 K=(D^4*G)/(8*(.425-D)^3*N)
205 C=(.425-D)/D
206 KS=1+.615/C
210 TAU=(8*(F0+K*DEL)*(.425-D)*KS)/(3.1416*D^3)
211 IF TAU>80000! THEN 230
220 PRINT D;N;F0;K;TAU
230 GOTO 90
250 END
```

VITA

David L. Conner was born in Knoxville, Tennessee on April 5, 1964. He graduated from Bearden High School in June 1982 and entered The University of Tennessee the following September. While at the University, he worked as a research assistant in the Agricultural Engineering Department, and received his Bachelor of Science degree in Mechanical Engineering in March 1987. He immediately entered The Graduate School, and worked as a graduate teaching assistant before receiving his Master of Science degree in May 1989.

The author is an associate member of the American Society of Mechanical Engineers and a member of the Pi Tau Sigma honorary society.